Modeling soil productivity in Montana using a Geographic Information System and existing data bases
by Ute Langner

A thesis submitted in partial fulfillment of the requirements for the degree of Master of Science in Earth Sciences
Montana State University

Abstract:
This research was undertaken to modify an existing productivity index requiring fewer inputs than other simulation models for use in semi-arid landscapes. The study was divided into two parts where the results of the first part were integrated into the second. In the first part, problems with yields published in modem U.S. soil surveys and the origins of the Montana Yield Model were reviewed. Recent soil survey applications of the Montana Yield Model incorporate very detailed soil inputs and very generalized climatological inputs. We used the ANUSPLIN interpolation techniques with climate station records, DEM data, and the ARC/INFO GIS to produce a series of improved consumptive water use maps. These data layers predicted noticeably different spatial and statistical patterns and magnitudes of consumptive water use across Montana compared with the original USDA-SCS map. The GIS-based maps offered the advantages of greater resolution, increased flexibility during classification, and repeatability. In the second part of the study, we chose a subset of soils from the Montana State Soil Geographic Database (STATSGO), assuming a mapping unit is comprised of one particular soil. We predicted yields and water deficit for those soils using a modified form of the current USDA-NRCS Montana Yield Model and GIS-based maps of growing season precipitation and consumptive water use. For each soil we extracted the corresponding yield-water deficit pairs and regressed them against each other. The results were used to generate a sufficiency factor for growing season water supply (deficit). A series of simulations were performed with the modified PI model to illustrate how impacts of soil erosion and/or climate change on productivity can be predicted in semi-arid landscapes. The type of model developed in this study can be used as a reconnaissance tool in semi-arid regions.

It has very modest data needs and a relatively simple conceptual basis (curves) and is easily implemented in GIS. This offers advantages in terms of data availability, ease of use, and clarity of output. Maps can be produced showing areas that are more/less vulnerable to productivity losses caused by climate change and/or accelerated erosion.

MODELING SOIL PRODUCTIVITY IN MONTANA USING A GEOGRAPHIC INFORMATION SYSTEM AND EXISTING DATA BASES

by

Ute Langner

A thesis submitted in partial fulfillment
of the requirements for the degree

of

Master of Science

in

Earth Sciences

MONTANA STATE UNIVERSITY-BOZEMAN
Bozeman, Montana

March 1998

APPROVAL

of a thesis submitted by

Ute Langner

This thesis has been read by each member of the thesis committee and has been found to be satisfactory regarding content, English usage, format, citations, bibliographic style, and consistency, and is ready for submission to the College of Graduate Studies

John P. Wilson (Graduate Committee, Chair)	John P. Wilson (Signature)	3/26/98 (Date)

Approved for the Department of Earth Sciences

Andrew Marcus (Department Head)	Andrew Marcus (Signature)	3/31/98 (Date)

Approved for the College of Graduate Studies

Joseph Fedock (Graduate Dean)	Joseph Fedock (Signature)	4/1/98 (Date)

STATEMENT OF PERMISSION TO USE

In presenting this thesis in partial fulfillment of the requirements for a master's degree at Montana State University-Bozeman, I agree that the Library shall make it available to borrowers under rules of the Library.

If I have indicated my intention to copyright this thesis by including a copyright notice page, copying is allowable only for scholarly purposes, consistent with "fair use" as prescribed in the U.S. Copyright Law. Requests for permission for extended quotation from or reproduction of this thesis in whole or in parts may be granted only by the copyright holder.

Signature Mike Langner

Date 3-31-98

ACKNOWLEDGMENTS

I would like to thank my advisor Dr. John P. Wilson for the invaluable assistance, innovative ideas, support and encouragement he has given me as a graduate student at Montana State University. I would also like to thank Dr. Andrew Marcus and Dr. William Kemp for serving on my graduate committee.

Financial support was provided by the Department of Earth Sciences and Geographic Information and Analysis Center at Montana State University. The climate data used in this study were prepared by Lisa Landenburger and the second author under Grant No. 91-34214-6056 from the Cooperative States Research Service of the United States Department of Agriculture. The USDA-NRCS Montana State Office provided a digital copy of the original USDA-SCS consumptive water use map and information on the Montana Yield Model. This project could not have been completed without the continued support of the GIAC staff, and fellow graduate students.

Finally, I would like to give special thanks to my family, Heiko and Adelheid, and to our parents for their loving support.

TABLE OF CONTENTS

LIST OF TABLES

LIST OF FIGURES

ABSTRACT

This research was undertaken to modify an existing productivity index requiring fewer inputs than other simulation models for use in semi-arid landscapes. The study was divided into two parts where the results of the first part were integrated into the second. In the first part, problems with yields published in modern U.S. soil surveys and the origins of the Montana Yield Model were reviewed. Recent soil survey applications of the Montana Yield Model incorporate very detailed soil inputs and very generalized climatological inputs. We used the ANUSPLIN interpolation techniques with climate station records, DEM data, and the ARC/INFO GIS to produce a series of improved consumptive water use maps. These data layers predicted noticeably different spatial and statistical patterns and magnitudes of consumptive water use across Montana compared with the original USDA-SCS map. The GIS-based maps offered the advantages of greater resolution, increased flexibility during classification, and repeatability. In the second part of the study, we chose a subset of soils from the Montana State Soil Geographic Database (STATSGO), assuming a mapping unit is comprised of one particular soil. We predicted yields and water deficit for those soils using a modified form of the current USDA-NRCS Montana Yield Model and GIS-based maps of growing season precipitation and consumptive water use. For each soil we extracted the corresponding yield-water deficit pairs and regressed them against each other. The results were used to generate a sufficiency factor for growing season water supply (deficit). A series of simulations were performed with the modified PI model to illustrate how impacts of soil erosion and/or climate change on productivity can be predicted in semi-arid landscapes. The type of model developed in this study can be used as a reconnaissance tool in semi-arid regions. It has very modest data needs and a relatively simple conceptual basis (curves) and is easily implemented in GIS. This offers advantages in terms of data availability, ease of use, and clarity of output. Maps can be produced showing areas that are more/less vulnerable to productivity losses caused by climate change and/or accelerated erosion.

CHAPTER 1

INTRODUCTION

Evaluation of the productivity of soils in relation to changes caused by soil erosion has been a research focus in the United States and other regions of the world for several decades. First, information on soil productivity has been and still is of economic and political interest, particularly to assess land for taxation, target agricultural support payments, or to evaluate the potential of land for development (Gersmehl and Brown, 1986). Second, changes in productivity have been related to soil erosion and a soil productivity index or rating could provide criteria necessary to maintain soil productivity at desired levels, delineate areas of critical erosion, and guide the selection of conservation practices or lands to be brought into cultivation (Pierce et al., 1984b). Spatial modeling and monitoring of soil productivity seems crucial in a state such as Montana where agricultural production is a major economic sector (64 percent of the state's total land is land in farms and ranches, about 25 percent is crop land; Montana Agricultural Statistics Service, 1996).

Numerous simulation models of varying complexity have been proposed to describe the effect of soil erosion on soil productivity (Gantzer and McCarty, 1987; Pierce, 1991; Olson et al., 1994). One of the simplest and yet most successful approaches to quantify the relationship between soil erosion and soil productivity was developed by

Pierce et al. (1983). The simplicity of their productivity index (PI) model may involve some loss in the description of the relationship between soil properties and productivity, and subsequently may reduce the model's accuracy. However, the PI model is attractive because it requires very few inputs, and, therefore, provides a less costly tool for analysis (Gantzer and McCarty, 1987) which is an important consideration for regions where data availability is sparse.

The PI is a simple algorithm based on the assumption that crop yield is a function of root growth, which in turn is controlled by the soil environment. It evaluates a soil's vulnerability by simulated removal of surface soil. The model treats PI as a function of pH, bulk density (BD), and available water holding capacity (AWC) which are considered the most important factors for crop production in the Corn Belt (where the model was developed from extensive data). The model's assumptions of constant climate and high level of management were intended to control the other important determinants of soil productivity (Pierce et al., 1984c). To account for a variable landscape and climatic differences across geographic regions, Pierce et al. (1984c) suggested adding a factor accounting for sufficiency of moisture supply. Other researchers also concluded that in semi-arid landscapes the performance of the PI approach probably depends on the ability to add a sufficiency factor for effective water supply (Rijsberman and Wolman, 1985; Gantzer and McCarty, 1987; Wilson et al., 1991). From a study of two soils with a high PI value, Pierce et al. (1984c) concluded that more work is needed to define the exact nature of the water supply sufficiency curve across a range in PI.

Currently, PI is calculated as the product of sufficiencies of three soil properties

(pH, bulk density (BD), and available water holding capacity (AWC)). The sufficiency of a particular soil factor is based on a response curve relating the measured value for that factor to a dimensionless sufficiency for root growth between 0.0 and 1.0. A water supply sufficiency curve could be generated (empirically) by relating soil specific water supply/deficit data to yield data (as a measure of productivity). Water supply/deficit could be estimated from precipitation and evapotranspiration information. Modified versions of the PI model (with altered model statements or new statements accounting for the response of crops to local soil characteristics) have been successfully applied to soils in Montana (Wilson et al., 1991, 1992). However, a water supply sufficiency curve has not been developed.

Having the goal of developing a water supply sufficiency curve for Montana soils in mind we analyzed data availability first. Spatially distributed data for the three soil factors in the PI model are provided through the State Soil Geographic Data Base (STATSGO; USDA-NRCS, 1994). Spatially distributed potential evapotranspiration and growing season precipitation data are needed for calculating water deficit. The latter can be produced from station data using the interpolation program ANUSPLIN developed by Hutchinson (1989a) and using the spatial analysis and map display capabilities of a GIS. Potential evapotranspiration information in past studies has been extracted from a very coarse consumptive water use map that was hand drawn (eyeballed) using data from approximately 90 climate stations across Montana (USDA-SCS, 1988). Alternatively, the spatial analysis and map display capabilities of a GIS provide the opportunity to produce a finer and more flexible map of consumptive water use (equivalent to potential

evapotranspiration). Spatially distributed yield data can be, in theory, extracted from county soil survey reports. However, analyses of the published yield data revealed that the yield tables must be treated as a very noisy set of data (Gersmehl and Brown, 1986) and that yield data from soil surveys generated between 1973 and 1988 (about 16 in Montana) should be treated as suspect and used with caution (Baker and Gersmehl, 1991). Fortunately, the Montana State Office of the NRCS has implemented a yield model based on field research by Brown and Carlson (1990) to generate more accurate non-irrigated small grain yield estimates. This yield model can be implemented in a GIS.

Therefore, the presented thesis has the following four goals. The first was to use existing data for the state of Montana to generate a sufficiency curve for growing season water supply that might be used in the PI model for semi-arid landscapes. A second goal was to test how a GIS can serve as an efficient tool to estimate necessary spatial data (potential evapotranspiration, growing season precipitation, water deficit, and yield) to solve this task and display results. A third goal of this thesis was to describe the construction of a more detailed GIS-based consumptive water use map. The final goal was to illustrate how the impacts of soil erosion and/or climate change on productivity can be predicted in semi-arid landscapes using the modified PI model.

This study involves a series of spatially and temporally distributed data layers and can only be conducted utilizing the spatial analysis and display capabilities of a GIS. It demonstrates one of the many applications of geographic information systems.

CHAPTER 2

GIS ESTIMATES OF CONSUMPTIVE WATER USE

BACKGROUND

Information on crop yields is fundamental for monitoring changes in productivity and land quality over time, targeting agricultural support payments and soil conservation programs, farm management studies, assessing land for taxation, and evaluating the viability of a mortgage proposal or the potential of a land development project (Larson et al., 1983; Gersmehl and Brown, 1986; Bryant and Lacewell, 1989; Dumanski and Onofrei, 1989). Yield estimates can be obtained from field measurements (e.g., Usery et al., 1995), statistical models (e.g., Brown and Carlson, 1990), and mechanistic crop growth simulation models (e.g., Carbone et al., 1996). Published county soil surveys in the United States have traditionally used one or more of these methods to estimate local yields for each of the soil mapping units delineated in these surveys.

Unfortunately, yield tables produced via any of these methods must be treated as very noisy data (Gersmehl and Brown, 1986). The quality of the yield estimates between and within counties is likely to vary greatly depending on the experience of the surveyor and the cooperation of farmers. Baker and Gersmehl (1991) analyzed published yield estimates for 30 soils in 233 U.S. counties to identify changes in crop yields along spatial gradients, and after compensating for the national trend of increasing yields over time,

they found that published estimates of crop yields in many regions have been essentially uniform since 1972 and show no spatial gradients. Baker and Gersmehl (1991) concluded that the compilers of these surveys have adopted the standardized yield estimates in the USDA-NRCS Mapping Unit Interpretation Record (MUIR) database (formerly known as the SOILS-5 database) rather than attempted to assess actual yields within a county. Hence, yield data from soil surveys completed between 1973 and 1988 should be used with caution (Baker and Gersmehl, 1991).

The problem of estimating yield is particularly acute in a state like Montana in which (1) there is a large crop land area (7,080,000 ha in 1992; Montana Agricultural Statistics Service, 1996), (2) there is a tremendous variety of soil and climatological resources (Montagne et al., 1982; Caprio and Nielsen, 1992), and (3) 18 of the 34 completed soil surveys that included yield estimates were published during the period 1973-1996. Fortunately, the Montana State Office of the USDA-NRCS has implemented a yield model based on experimental research by Brown and Carlson (1990) to help overcome these problems and generate more accurate estimates of non-irrigated small grain yield. This new model is driven mostly by hydrological parameters, because water is the most important factor limiting crop production in Montana.

Brown and Carlson (1990) measured stored soil water, precipitation and grain yield data for scattered locations in north-central Montana between 1982-1989. These data were used to develop linear regression equations that related crop yield to evapotranspiration (ET). ET was defined as the sum of measured initial stored soil water (or plant available water at seeding) and growing season rainfall. Regression coefficients

(R^2 values) of 0.73, 0.77, 0.84, and 0.87 were achieved for high yielding cultivars of oats, barley, spring wheat, and winter wheat, respectively. Brown and Carlson (1990) extended the north-central Montana ET-yield equations to the other crop producing areas of the state using consumptive water use data (FIGURE 1; USDA-Soil Conservation Service, 1988).

Doorenbos and Pruitt (1977) defined consumptive use (CU) as 'the amount of water potentially required to meet the evapotranspiration needs of vegetative areas so that plant production is not limited by lack of water.' This is equivalent to the amount of water that plants will use in transpiration and in building cell tissue, plus that evaporated from adjacent soil and plant surfaces (Blaney and Criddle, 1950; USDA Soil Conservation Service, 1988; U.S. Soil Conservation Service, 1993). Brown and Carlson (1990) used the CU value estimated for north central Montana (17.36 inches) as the ET in their north-central MT regression equations for each crop, and used the resulting yields and CU values for other map areas to estimate slope parameters for the respective crop regression equations in the other consumptive water use areas (map classes 1, 3, and 4, respectively). Next, they used these regression equations to develop yield tables for winter and spring wheat, oats, and barley in each consumptive water use area, based on the potential of the crop relative to available moisture (stored soil water plus growing season rainfall). The USDA-NRCS Montana Yield Model calculates the plant available water as the sum of soil water holding capacity, growing season rainfall (May 1 - July 31), and several adjustment factors (Hansen, personal communication, 1997). Adjustments account for the effects of slope, soil particle size, water table depth and

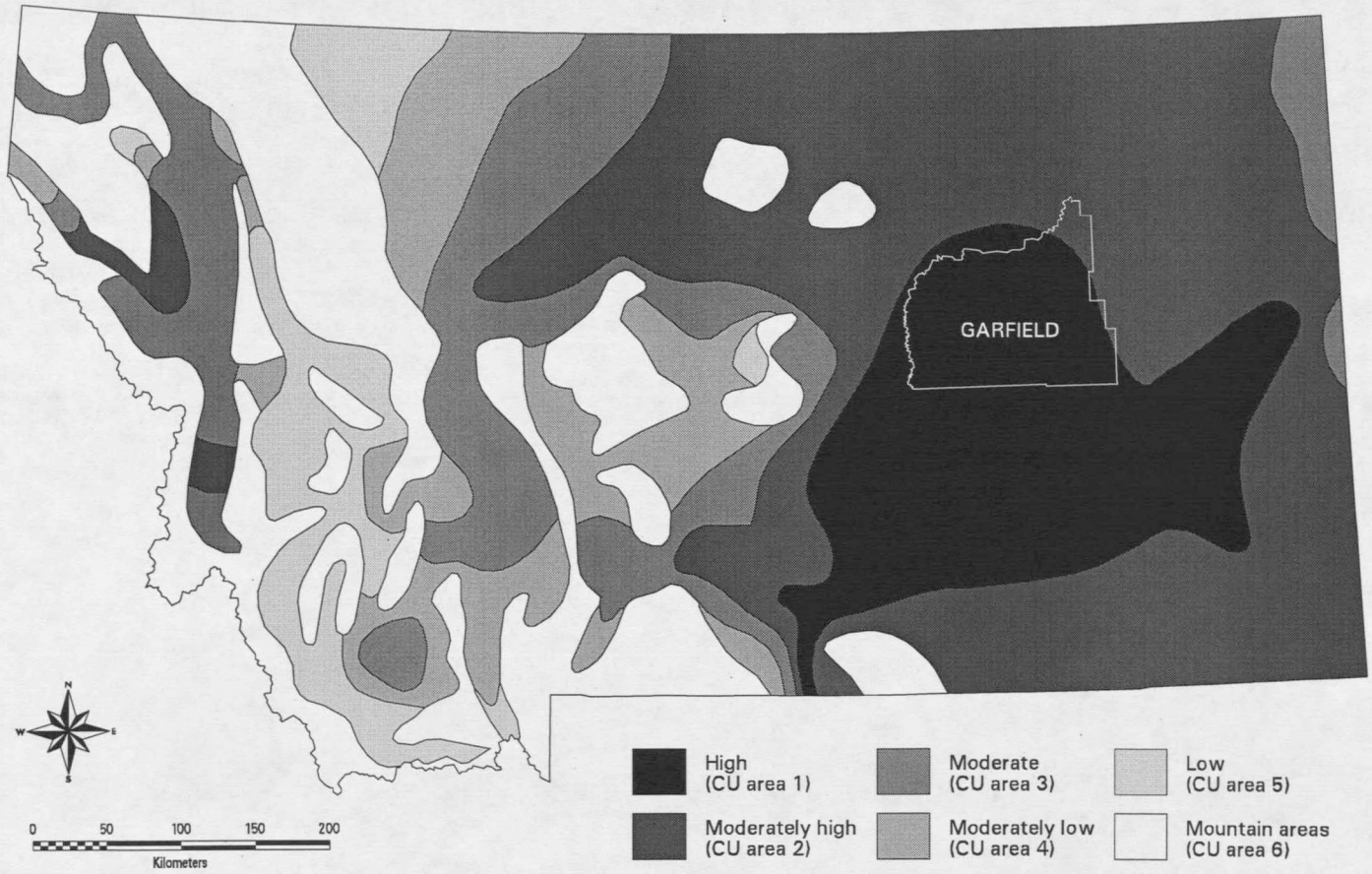

FIGURE 1. Irrigation climate areas delineated by USDA-Soil Conservation Service (1988) by (a) applying the TR-21 computer program to 90 sites with climate data, and (b) dividing the state into six consumptive water use areas of approximately equal size. The boundary of Garfield County, one of 56 counties in the State of Montana, is also shown as it is referenced later in the text.

ponding, soil organic matter content, lime and sodium content in the soil, and length of frost free season (TABLE 1). The model utilizes soil data from the digital MUIR data base compiled by the USDA-NRCS Montana State Office and growing season rainfall totals provided by the user. The adjusted plant available water is then linked to the crop yield equations developed by Brown and Carlson (1990). These equations predict higher yields in areas of lower consumptive water use for a specified quantity of water since plants in areas of high consumptive use will be subjected to greater water stress (Brown and Carlson, 1990). Also, yield estimates for soil survey reports assume: (1) a moisture depth of 40 inches at the beginning of the growing season (this corresponds to the maximum moisture level that is accumulated after summer fallow; Hansen, personal communication, 1997), and (2) a high management level (by which plants grow at their physiological optimum). However, both of these assumptions may be varied for other model runs to reflect soil profiles that are not fully charged at the beginning of the growing season and other management levels.

The new yield model combines very detailed soil inputs with very generalized climate inputs. Model runs for Garfield County, for example, would combine soil interpretation records for 93 soil map units and two consumptive water use map units (FIGURE 1). The current CU map shows broad spatial patterns based on six classes. This map was prepared manually some years ago (1986) and gives the misleading impression that uniform conditions are likely to occur within each of the consumptive water use areas. Geographic Information Systems (GIS), with their ability to manipulate and display multiple data layers, can provide a more systematic and dynamic approach to zoning than

TABLE 1. Yield relationships incorporated in USDA-NRCS Montana Yield Model.

Basic model:

$$Yield = GYC * (AWC + GSP + adjustments) * ffs + IYP$$

where *Yield* is yield in bushels per acre, *GYC* is a grain yield coefficient which varies with crop and consumptive water use area, *AWC* is water holding capacity in inches, and *GSP* is growing season precipitation in inches. *Adjustments* are calculated in inches for slope, soil particle size, water table depth and ponding, organic matter content, lime content, and sodium content. *ffs* is a short frost free season factor, and *IYP* is the initial yield point which varies with crop and consumptive water use area.

Rules for calculating adjustments and short frost free season factor:

(1) if particle size = group A (Clayey):
- if slope high > 8 and slope high ≤ 15 then adjustment = -1
- if slope high > 15 and slope high ≤ 25 then adjustment = -2
- if slope high > 25 then adjustment = -3.5

if particle size = group B (Loamy)
- if slope high > 8 and slope high ≤ 15 then adjustment = -0.5
- if slope high > 15 and slope high ≤ 25 then adjustment = -1.5
- if slope high > 25 then adjustment = -2.5

if particle size = group C (Sandy)
- if slope high > 15 and slope high ≤ 25 then adjustment = -0.5
- if slope high > 25 then adjustment = -2.5

where *slope high* is the maximum value for the range of slope of a soil component within a map unit in percent

(2) if water table depth low ≥ 2 and water table depth low ≤ 4 then adjustment = 1

if water table depth low ≥ 4 and water table depth low ≤ 5 then adjustment = 0.5

if ponding depth low < 0 then adjustment = -3

where *water table depth low* is the minimum value for the range in depth to the seasonally high water table during the months specified, in inches, and *ponding depth* low is the minimum value for the range in depth of surface water ponding on the soil in inches.

(3) if the Subgroup category = 'pachic' or 'pachic udic' or ' pachic ultic' or 'pachic vitric' or 'argic pachic' or 'aridic pachic' or 'calcic pachic' or 'cumulic' then adjustment = 1

where *Subgroup* is a category in the U.S. Soil Taxonomy (USDA-NRCS, 1994).

(4) if in upper most soil horizon $CaCO_3$ high > 5 or its wind erodibility group = 'surface texture = calcareous; L/SIL/CL, SICL; percent aggregates = 25; wind erodibility index = 86 t/a/y' then adjustment = -0.5
if Mineralogy = 'carbonatic' then adjustment = -1

where *$CaCO_3$ high* is the maximum value for the range of calcium carbonate in the specified soil layer or horizon in percent, *wind erodibility group* (weg) is the weg assigned to the soil layer or horizon, and *Mineralogy* is the mineralogy class of the Family category of the Taxonomic Classification (USDA-NRCS, 1994).

(5) (a) if in upper most soil horizon the Sodium Absorption Ratio high > 13 then adjustment = -5
(b) if depth of second soil horizon low ≤ 12 and its Sodium Absorption Ratio high ≥ 13 and the adjustment in (a) = -5 then adjustment = -1.5
(c) if adjustment in (a) = -5 and Great Group category = 'Natraqualfs' or 'Natriboralfs' or 'Natrudalfs' or ' Natrustalfs' or 'Natrixeralfs' or 'Natralbols' or 'Natraquolls' or 'Natriborolls' or 'Natrustolls' or 'Natrixerolls' or 'Natraquerts' or 'Natrargids' then adjustment = -1.5
(d) if adjustment in (a) = -5 and Subgroup category = 'natric' then adjustment = -1.5

where *Sodium Absorption Ratio high* is the maximum value for the range in Sodium Absorption Ratio for the soil layer or horizon, *depth of second soil horizon low* is the depth to the upper boundary of the soil layer or horizon in inches, and *Great Group* is a category in the U.S. Soil Taxonomy (USDA-NRCS, 1994).

(6) if frost free season = 70-90 days then ffs-factor = 0.7
if adjustment in (2) = 1 and ffs-factor = 0.7 then ffs-factor = 0.6

the traditional, somewhat limiting, cartographic approach (Corbett and Carter, 1996; Custer et al., 1996). The overall aim of this paper is to illustrate how the use of GIS can help to prepare more flexible and accurate maps. The specific objectives are to: (1) describe the construction of a GIS-based consumptive water use map, and (2) demonstrate how GIS can be utilized to estimate soil and climatological traits that contribute to differences in crop yields.

METHODS AND DATA SOURCES

The consumptive water use map currently used by the USDA-NRCS (FIGURE 1) was developed using the Blaney-Criddle method (Blaney and Criddle, 1950; USDA-Soil Conservation Service, 1988; U.S. Soil Conservation Service, 1993). We utilized the same method with the ARC/INFO GIS (Environmental Systems Research Institute, Inc., Redlands, CA) to prepare a new series of maps that we compared with a digital copy of the original map.

The Blaney-Criddle Consumptive Use Method

Spatially distributed growing season consumptive water use (*CU*) values were computed in inches for Montana spring grains as follows:

$$CU = K \sum_{i=1}^{3} p_i \, t_i \, / \, 100 \qquad (1)$$

where: K is an empirical consumptive-use crop coefficient for the growing season, p_i is the monthly percentage of annual daylight hours, t_i is the mean monthly air temperature in degrees Fahrenheit, and $i = 1, 2, 3$ for May, June, July (i.e., the growing season for spring grain in Montana).

Consumptive-use crop coefficients have been determined experimentally at numerous localities for most crops grown in the western U.S. For small grains with a 3 month growing season, the empirical consumptive-use crop coefficient for the growing season (K) equals 0.75 in humid areas and 0.85 in arid areas (U.S. Soil Conservation Service, 1993). The latter value was used in this study. Spatially distributed temperature and daylight grids were prepared using the methods discussed in the next two sections.

Preparation of Mean Monthly Temperature Grids

Gridded mean monthly temperature estimates were generated with ANUSPLIN (Hutchinson, 1989a). This model, which incorporates two separate programs (SPLINA, LAPGRID) that combine Laplacian thin plate smoothing splines with location (latitude, longitude) and elevation (in kilometers above sea level), was used to estimate mean monthly minimum and maximum temperatures for the period 1961-90. Stations from adjacent provinces and states were included to account for edge effects and stations with longer records were weighted more heavily than stations with shorter or incomplete records in the analysis outlined below.

Climate data for 954 stations in Montana and parts of Alberta, Saskatchewan,

North Dakota, South Dakota, Wyoming, and Idaho for the period 1961-90 were used in SPLINA to generate a surface coefficients file and numerous diagnostics. Stations with shorter records and/or missing data were weighted using $1/n$ where n is the number of months of record (Hutchinson, 1995). The degree of smoothing is automatically determined in SPLINA by minimizing the predictive error of the fitted surface with generalized cross validation (GCV). The GCV is calculated by removing each data point (climate station) in turn and summing the square of the discrepancy of each omitted data point from the surface fitted to the remainder of the data points. The final GCV and other diagnostics (list of residuals and other summary statistics) were used to find and correct errors in input data and to evaluate the efficiency of the final surface (Hutchinson, 1991).

The second program called LAPGRID used the surface coefficients file with a digital elevation model (DEM) to interpolate mean monthly minimum and maximum temperatures at each grid cell across the study area. Grid cells measuring 50 arc seconds (approximately 0.6 x 0.9 km) on a side were generated from the United States Geological Survey 3 arc-second DEM with ANUDEM (Hutchinson, 1989b) and used with LAPGRID. The mean monthly minimum and mean monthly maximum temperature grids for May, June, and July were copied to ARC/INFO and the mean monthly average temperature was calculated for each grid cell in each month.

Preparation of Relative Daylight Length Grids

Grids showing the monthly percentage of annual daylight hours (p_i) were also

generated in ARC/INFO from ASCII files containing interpolated *p*-values for each growing season month for the latitudes of the grid cell midpoints. Original *p*-values were taken from TABLE 2 published in the National Engineering Handbook (U.S. Soil Conservation Service, 1993) and *p*-values for the intermediate latitudes were interpolated in a spreadsheet using a linear equation of the form $y = a+bx$, where x are the latitudes and y are the *p*-values. The slope (b) and intercept (a) were calculated for each pair of consecutive latitude values in TABLE 2 so that five different equations were used in the interpolation process. The relative daylight length grids were generated at the same orientation and resolution as the temperature grids to facilitate model implementation.

TABLE 2. Monthly percentage of annual daylight hours for latitudes of interest (from USDA-SCS, 1993, p. 2-228).

Latitude N	May	June	July
49°	10.60	10.82	10.90
48°	10.52	10.72	10.81
47°	10.45	10.63	10.73
46°	10.38	10.53	10.65
45°	10.31	10.46	10.57
44°	10.25	10.39	10.49

Map Classification

We developed the classification scheme summarized in TABLE 3 to group the CU grid values into regions as in FIGURE 1. We inferred class limits for five

consumptive use regions from values for the consumptive use areas 1 through 4 published by Brown and Carlson (1990), assuming that the given values were means and that the values within the classes were normally distributed. Class limits between two given values were calculated as the mean of the two for consumptive use classes 1 through 4 (TABLE 3). To determine the lower limit of class 4, we subtracted the difference between the published mean values of class 3 and 4 from the published consumptive use value of class 4 which gave us an extrapolated mean value for class 5 (14.45 inches). The mean of the consumptive use values of class 4 and 5 constitutes the lower limit of class 4. We combined classes 5 and 6 of the original USDA-SCS consumptive use map (FIGURE 1) to facilitate comparison of the resulting maps since the conditions represented by these classes are not suited to cereal crops.

TABLE 3. Class limits used to generate new consumptive use estimates and maps.

CU class	Published CU value	Class limits
1 - High	18.46	≥ 17.91
2 - Moderately high	17.36	$16.575 \leq CU < 17.91$
3 - Moderate	15.79	$15.455 \leq CU < 16.575$
4 - Moderately low	15.12	$14.785 \leq CU < 15.455$
5 - Low and Mountains	14.45	<14.785

Three additional maps were prepared to evaluate the sensitivity of our new CU map to the grid (map) resolution and/or method of classification. We applied two different 3 by 3 moving window filters to our new CU grid to smooth the differences

between neighboring cell values and evaluate the effect of level of smoothing on map classification. The first filter applied a weight of 0.8 to the center cell and a weight of 0.025 to the eight neighboring cells. The second filter applied a weight of 0.6 to the center cell and a weight of 0.05 to the eight neighboring cells. The two resulting grids CUF1 and CUF2 were reclassified using the same classification scheme as above (TABLE 3). For the third map, we reclassified our CU grid into a grid (CUPR) with six classes such that the same proportion of cells was assigned to each of the classes as in the USDA-SCS consumptive use map. This particular map was developed to evaluate whether or not the differences between our resulting map of consumptive use regions and the original USDA-SCS consumptive use map might be explained by disparities in the magnitude of the estimates.

Comparison of Map Products

The original USDA-SCS consumptive use map (FIGURE 1) was converted into a grid to facilitate cell by cell comparison of the two maps in the ARC/INFO GIS. Overlaying all resulting grids (CU, CUF1, CUF2, CUPR) with the original map revealed the differences in the classification of cells between the four new maps of consumptive use regions and the original USDA-SCS consumptive water use map. The final maps reproduced in this paper (FIGURES 1-5) use the Albers equal area projection in place of the geographic coordinates (decimal degrees) that were used for the database development and overlay analysis.

RESULTS AND DISCUSSION

In the original USDA-SCS consumptive water use map (FIGURE 1) classes consist of one contiguous or several disjunct areas (referred to as polygons hereafter). Small polygons tend to concentrate in the mountainous area (western part) of the state, particularly west of the continental divide. These polygons were classified as consumptive water use classes 4-6. Large polygons representing consumptive water use classes 1-3 occur in the eastern half of Montana.

The original map class boundaries follow major landform features (FIGURE 2). The boundary of consumptive use class 1, the large polygon in the center of eastern Montana, follows the Lower Yellowstone Valley between the Pryor Mountains and Beartooth Plateau in the south, the Musselshell River Valley to the west, the Missouri River to the north, and Yellowstone and Powder River Valleys to the east. Consumptive use class 2 is dominated by one large polygon that covers most of the remainder of the eastern half of the state. The two outstanding circles in the northwest of consumptive use class 2 coincide with the Bear Paw and Little Rocky Mountains (consumptive use class 6). The Judith, Big Snowy, and Crazy Mountains delineate the western margin of consumptive use area 2, and the Beartooth Plateau, Pryor and Bighorn Mountains mark its southern boundary. Consumptive use class 3 consists of two polygons along the eastern border of the state, one long but narrow polygon that marks the plains-mountain margin and the Missouri River Valley to the west of CU area 2, and three polygons west of the continental divide that follow the Kootenai and Stillwater River Valleys in the

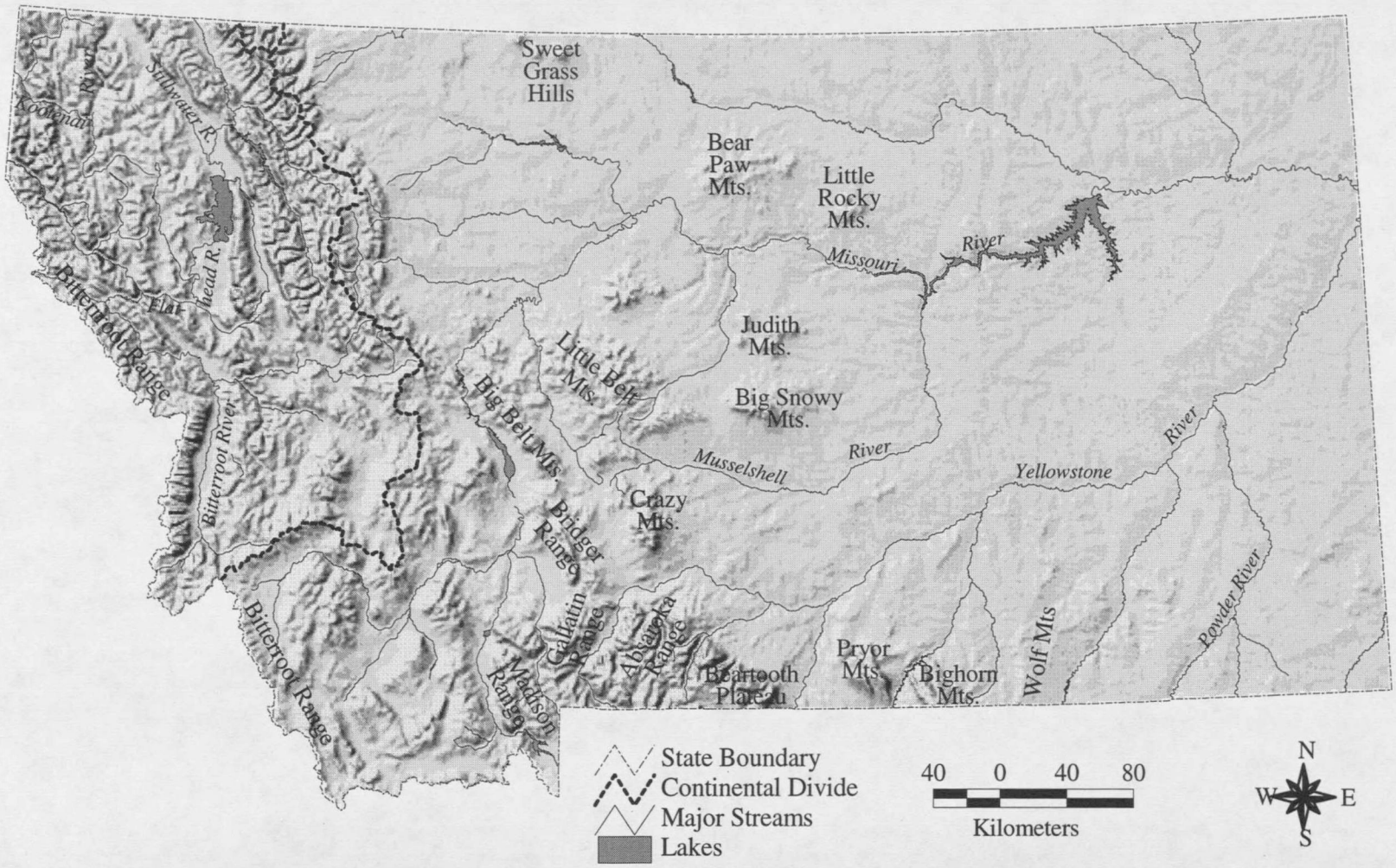

FIGURE 2. Physiographic map of Montana, constructed from series of maps at http://nris.mt.gov/gis/mtmaps.html.

north and Flathead and Bitterroot River Valleys in the south. Consumptive use class 4 is represented by several small polygons that follow the plains-mountain margin and a series of mountain valleys. Consumptive use class 5 displays a similar pattern, and most of these polygons are located west of the continental divide. Consumptive use class 6 represents high mountains with individual polygons identifying mountain ranges such as the Bitterroot Range at the western border of Montana, the Madison, Gallatin, Bridger Ranges and the Big Belt Mountains in south-central Montana, the Absaroka Range, Beartooth Plateau, and Pryor and Bighorn Mountains at the south border of Montana, etc. The first four columns in TABLE 4 summarize the number of polygons, GIS grid cells, and areal distribution of the consumptive use classes in the original USDA-SCS CU map.

TABLE 4. Consumptive use areas delineated in original USDA-SCS consumptive water use map (FIGURE 1) and in the GIS-based consumptive water use map (FIGURE 3).

Consumptive Use Class	FIGURE 1			FIGURE 3	
	Number of Polygons	Number of Pixels	Percent of State Covered	Number of Pixels	Percent of State Covered
High (CU area 1)	1	92844	14.3	2	0
Moderately high (CU area 2)	3	222965	34.3	289068	44.5
Moderate (CU area 3)	7	95760	14.8	144997	22.3
Moderately low (CU area 4)	11	59346	9.1	52974	8.2
Low (CU area 5)	5	38899	6	162107	25
Mountains (CU area 6)	17	139334	21.5		

We compared the original USDA-SCS consumptive water use map (FIGURE 1)

to our consumptive water use grid reclassified into the same classes as the original map with the exception of classes 5 and 6 which we combined into one class (FIGURE 3). The comparison of the two maps revealed a difference in the statistical distribution (TABLE 4) and spatial pattern of consumptive water use classes across Montana (FIGURE 3). On our GIS generated map only two grid cells in north-west Montana were classified in the highest consumptive use class. Eastern Montana in the new map was assigned to consumptive use class 2. Consumptive use class 3 surrounds class 2, coinciding with higher elevation features to the west, south and north of class 2. Consumptive use area 4 constitutes a narrow band surrounding mountains that were assigned to consumptive water use classes 5 and 6 in the original map and class 5 in the new maps. In summary, the outline of the original consumptive use class 1 and the northern, eastern and southern borders of consumptive use class 3 are not visible in our grid (map). Consumptive use area 4 covers a slightly smaller area than in the original map. The Sweet Grass Hills in the north and Wolf Mountains in the south stand out in our consumptive use grid in addition to the mountain areas in the original map. The last two columns in TABLE 4 show the areal distribution of the consumptive water use classes based on the GIS-based grid reproduced in FIGURE 3.

The distribution of grid cells in our final CU grid (FIGURE 3) across each of the original USDA-SCS polygons is summarized in TABLE 5. The first column indicates that each row denotes one polygon in the original USDA-SCS consumptive water use map. The second and third columns display the CU class and number of GIS grid cells in each USDA-SCS polygon (FIGURE 1). Columns four through eight show how many of

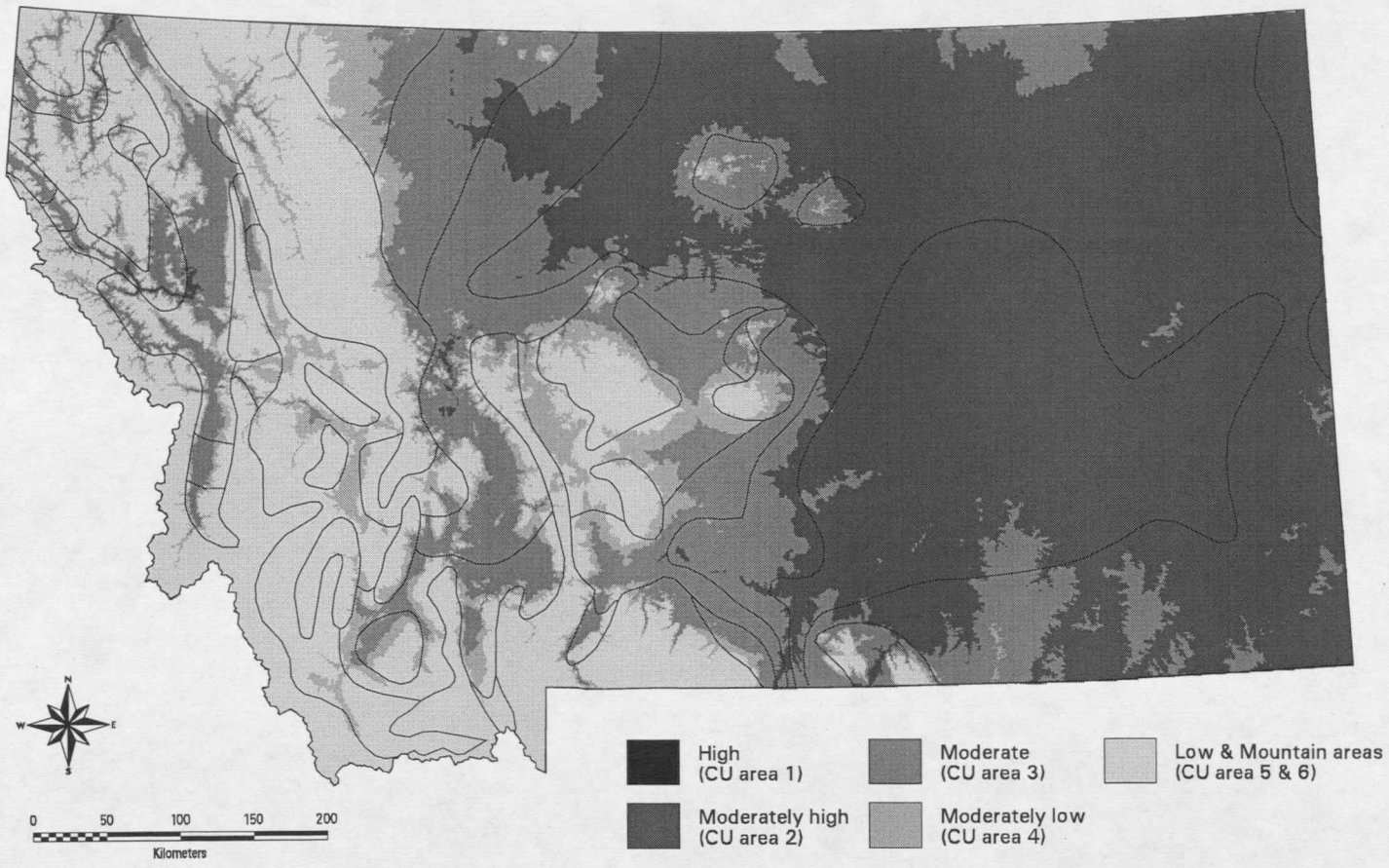

FIGURE 3. Consumptive water use map generated with ANUSPLIN temperature surface and Blaney-Criddle method. Lines indicate boundaries for consumptive water use areas shown in FIGURE 1.

the grid cells in the original USDA-SCS polygon are assigned to classes 1-5 in our GIS-based consumptive use grid (FIGURE 3). The ninth and last column lists the percent agreement per USDA-SCS polygon, indicating how many cells per polygon are assigned to the same class in both the GIS-based and USDA-SCS consumptive water use maps. The final row of TABLE 5 indicates the percentage of cells per consumptive use area assigned to the same class in the two consumptive use maps. The number in the last row of the last column of the table shows the overall level of agreement between the original USDA-SCS and the GIS-based consumptive use maps, describing the percentage of cells in Montana that were assigned to the same classes in the two maps. This type of table was constructed for all four overlays (CU, CUF1, CUF2, CUPR).

TABLE 5. Distribution of grid cells in our final CU grid (FIGURE 3) per polygon in the original USDA-SCS consumptive use map (FIGURE 1). Bold numbers in columns 4-8 show number of cells that fall in same classes in two maps.

SCS polygon	SCS class	Cell count per polygon	Cell count per SCS polygon in					Percent agreement per polygon
			class 1	class 2	class 3	class 4	class 5	
1	6	4289			382	732	**3175**	74
2	3	22127		379	**10207**	4347	7194	46
3	6	36561			1522	3960	**31079**	85
4	5	9642			2751	4829	**2062**	21
5	4	18827		1099	15841	**1716**	171	9
6	3	60628		12160	**39789**	5010	3669	66
7	2	217029	2	**177176**	39423	359	69	82
8	3	6824		6824	**0**			0
9	6	12117			914	1889	**9314**	77
10	4	636			294	**90**	252	14
11	6	3763		22	3094	584	**63**	2
12	5	683			50	245	**388**	57
13	4	464				**130**	334	28
14	4	1146			491	**227**	428	20

SCS polygon	SCS class	Cell count per polygon	Cell count per SCS polygon in					Percent agreement per polygon
			class 1	class 2	class 3	class 4	class 5	
15	6	1915		543	1245	122	**5**	0
16	4	556			240	**170**	146	31
17	6	2937			63	366	**2508**	85
18	6	23313			310	1404	**21599**	93
19	3	735			**348**	126	261	47
21	1	92844	**0**	89204	3640			0
22	2	4404		**228**	2257	776	1143	5
23	5	26719			472	5173	**21074**	79
24	6	9858		5	1226	2319	**6308**	64
25	4	17158			6771	**6763**	3624	39
26	6	3300		3	1035	1100	**1162**	35
27	3	1021		1021	**0**			0
29	5	1046			659	362	**25**	2
30	4	1210			110	**573**	527	47
31	6	1525				79	**1446**	95
32	6	1248				75	**1173**	94
33	2	1532		**0**	713	232	587	0
34	4	4210			300	**817**	3093	19
35	6	2463			11	396	**2056**	83
36	3	1573			**245**	221	1107	16
37	6	1848			232	409	**1207**	65
38	4	12167			4359	**3001**	4807	25
39	6	3384				202	**3182**	94
40	6	5073			3	161	**4909**	97
41	6	21679			1739	2134	**17806**	82
42	4	1809		30	1270	**384**	125	21
43	4	1163			465	**82**	616	7
44	3	2851			**756**	722	1373	27
45	6	4060		374	1769	662	**1255**	31
46	5	808				24	**784**	97
Total percent agreement			0.0	61.4	28.4	26.3	77.9	*57.8*

For our final CU grid we constructed a confusion matrix (TABLE 6). It shows what classes of the original consumptive water use map were confused with what classes of our GIS-based CU grid. Most grid cells of consumptive water use class 1 of the

TABLE 6. Confusion matrix for grid cells of the original CU map (FIGURE 1) versus our final CU grid (FIGURE 3).

		CU class in original map (FIGURE 1)							
		1	2	3	4	5	6	Total	Percent correct
CU class in GIS-based map (FIGURE 3)	1	**0**	2	0	0	0	0	2	0
	2	89204	**177404**	20384	1129	0	947	289068	61.4
	3	3640	42393	**51345**	30141	3933	13545	144997	35.4
	4	0	1367	10427	**13953**	10633	16594	52974	26.3
	5	0	1799	13604	14123	**24333**	**106192**	160051	81.6
Total		92844	222965	95760	59346	38899	137278	647092	
Percent correct		0	79.6	53.6	23.5		74.1		*57.7*

original CU map were assigned to class 2 in our CU grid. About 80 percent of the grid cells from the original consumptive water use class 2 were assigned to class 2 in our CU grid, and most of the other 20 percent were assigned to class 3 in our map. About 54 percent of the grid cells are assigned to CU class 3 in both compared consumptive water use maps. CU class 4 is classified very differently in both maps, and 75 percent of the grid cells are assigned to classes other than CU class 4. Approximately 75 percent of the grid cells of the original CU classes 5 and 6 are assigned to the combined CU class 5 in our final CU grid, however, about 10 percent are classified into classes 2 and 3. Overall,

the results show a different pattern in classification.

The percent agreement per polygon (TABLE 5) and confusion matrix (TABLE 6) both provide measures of how well the GIS-based class delineation of consumptive use matched the polygon boundaries outlined in the USDA-SCS map. The percent agreement per polygon varies from 0 to almost 100 percent. For all four overlays the best agreement can be found among the polygons which belonged to classes five and six (low consumptive water use areas in mountain areas) in the original USDA-SCS map which were combined as class five in the GIS-based consumptive use map (TABLE 3). The percent agreement between the new CU grid and original map was less than 50 percent in 20 of the 22 polygons assigned to classes 1-4 (TABLE 5). Similar results were generated when the other GIS-based maps were combined with the USDA-SCS map (TABLE 7). These results have important implications for the Montana Yield Model because these polygons of low agreement incorporate the major crop producing areas in the state. Inaccurate polygon delineation and therefore class assignment may have a substantial impact on the accuracy of the model's yield predictions.

The percent agreement per polygon for the CU, CUF1, and CUF2 overlays differed by less than 0.4 percent (TABLE 7). This result suggests that the difference between the two consumptive water use maps were not caused by discrepancies in resolution that could be resolved with filters operating in a 3 by 3 moving window. The percent agreement per polygon for the CUPR (proportional reclassification) and CU overlays were higher over the first four classes (as expected) since the same proportions were used in place of the predicted class limits (TABLE 3) to assign classes on the CUPR

TABLE 7. Percent agreement per class and map comparing four GIS-based maps and the original USDA-SCS consumptive water use map (FIGURE 1).

Overlay	Percent agreement per class					Overall percent agreement
	class 1	class 2	class 3	class 4	class 5	
CU	0.00	61.37	28.37	26.34	77.89	57.81
CUF1	0.00	61.36	28.52	26.41	77.94	57.88
CUF2	0.00	61.42	28.67	26.55	77.55	57.95
CUPR	45.55	65.42	32.48	29.66	75.88	59.61

map (TABLE 7). FIGURE 4 illustrates the spatial pattern of the percent agreement per polygon for the CU overlay. The large (dark-shaded) polygon in the southeast corner of the state delineates the polygon that was classified as consumptive water use class 1 in the original USDA-SCS CU map. This area was not distinguished from surrounding areas in the GIS-based maps. A visual comparison of this map and a physiographic map of Montana reveals that most of the smaller dark-shaded areas of low agreement follow river valleys. The two small dark-shaded polygons to the north-central part of the map represent the Bear Paw and Little Rocky Mountains which are not of much agricultural interest. FIGURE 4 illustrates low agreement in most of the dryland farming areas and higher agreement in non-arable areas. The results show that utilizing the different maps may have a substantial impact on the accuracy of the yield predictions from the Montana Yield Model.

The results presented thus far show that GIS maps predict different spatial patterns and magnitudes of consumptive water use. The larger number of climate stations and DEM grid points coupled with the interpolation methods that were used to generate

FIGURE 4. Spatial distribution of percent agreement per polygon between the final GIS-based and the original USDA-SCS consumptive water use maps.

these estimates suggests that the new maps provide a superior description of consumptive water use across the state of Montana. The GIS methods offer at least five additional advantages. First, the GIS-based maps provide spatially distributed estimates of potential evapotranspiration that allow the user to perform the final classification (FIGURE 5). Second, the GIS method can be used to produce temporal series of consumptive water use maps accounting for varying growing season lengths of different crops, or to provide monthly estimates of potential evapotranspiration. Third, evapotranspiration was estimated at a finer spatial resolution than in the original USDA-SCS map. Data can be generated for different resolutions, either by aggregating to the desired resolution or by specifying the desired cell size when interpolating temperature surfaces in ANUSPLIN. Fourth, the GIS-based methods are repeatable and could be applied to prepare maps for other areas. Finally, the GIS-based consumptive use map (or any of the input grids) can be combined with other GIS layers as they become available as well. The county soil survey maps are being digitized and may be available within the next decade. These fine resolution data, for example, could easily be combined with the information on potential evapotranspiration and used to generate more specific and more accurate yield estimates in the future.

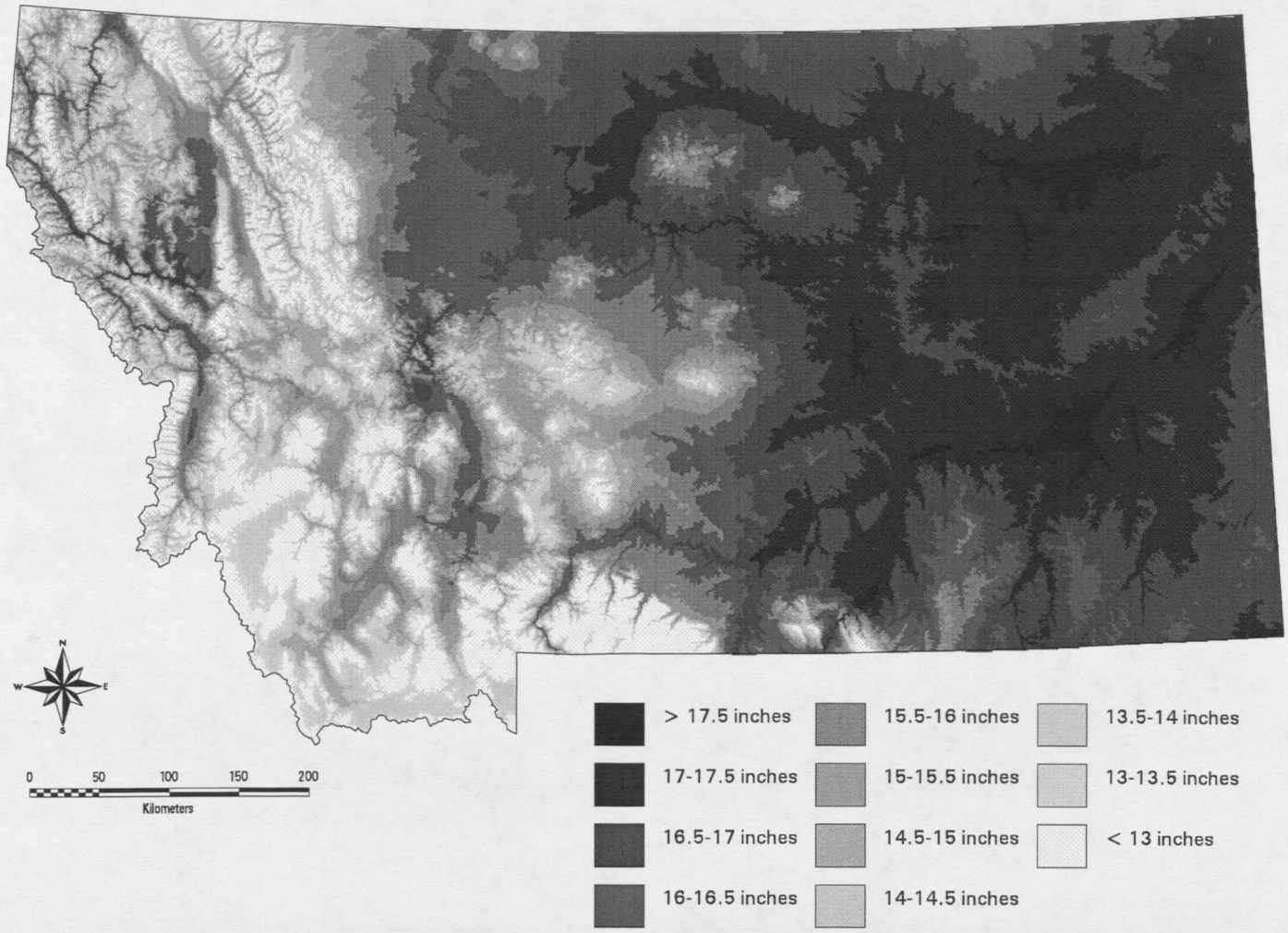

FIGURE 5. The GIS-based consumptive water use map classified into classes representing 0.5 inch increments.

CONCLUSIONS

The problems inherent in the yield tables published in modern soil surveys in the U.S. and the origins of the Montana Yield Model were reviewed. Recent soil survey applications of this model incorporate very detailed soil inputs and very generalized climatological inputs. The consumptive water use map (FIGURE 1) used in this model exemplifies many of the map products that were produced prior to the widespread adoption and use of GIS and related geographic information technologies.

We used the ANUSPLIN interpolation techniques with climate station records, digital elevation model data, and the ARC/INFO GIS to produce a series of new and improved consumptive water use maps. These maps or data layers predicted noticeably different patterns of consumptive water use compared with the original USDA-SCS map. The GIS-based maps also offered the advantages of greater resolution, increased flexibility during classification, and repeatability. Overall, these results show how GIS can be used to improve models, and they highlight the challenges of using highly generalized cartographic products with more detailed inputs in modern resource assessments.

CHAPTER 3

A SIMPLE PRODUCTIVITY INDEX FOR SEMI-ARID LANDSCAPES

BACKGROUND

The Productivity Index (PI) was developed to quantify the relationship between soil erosion and crop productivity. The PI model is based on the assumption that crop yield is a function of root growth, including rooting depth, which in turn is controlled by the soil environment. It evaluates a soil's vulnerability by simulated removal of surface soil. The model was developed by Neill (1979), and later modified by Kiniry et al. (1983). Pierce et al. (1983, 1984a, 1984b, 1984c) proposed a more generalized form of the model that incorporated some additional concepts based primarily on soil textural classes and used the SOILS-5 database developed by the United States Department of Agriculture's Soil Conservation Service (Reybold and TeSelle, 1989). This particular form of the model treated PI as a function of pH, bulk density (BD), and available water holding capacity (AWC) as follows:

$$PI = \sum_{i=1}^{n} A_i \; C_i \; D_i \; WF_i \qquad (2)$$

where A_i is the sufficiency of AWC, C_i is the sufficiency of BD (adjusted for permeability), D_i is the sufficiency of pH, WF_i is a weighting factor, and n is the number

of soil layers. The sufficiency of a particular soil factor is based on a response curve relating the measured value for that factor to a dimensionless sufficiency for root growth between 0.0 and 1.0 (FIGURE 6).

Numerous applications have demonstrated that spatial variations in PI matched spatial variations in measured soil losses or measured (published) yields in the U.S. Corn Belt. Pierce et al. (1983) found that the regression of yield for soils in southeastern Minnesota (as reported in the national SOILS-5 database) on PI accounted for 71 percent of the variability in corn yield. Pierce et al. (1984a) evaluated model performance in several counties in Minnesota using the relationship between yields as reported in county soil surveys and PI, and the relationship between Minnesota Crop Equivalent Rating (CER) and PI. The final R^2 ranged from 0.63 to 0.71 and intermediate values were increased by 26 percent on average when Histosols, frequently flooded and depressional soils, and soils with slopes exceeding 6 percent were excluded.

Gantzer and McCarty (1987) found that PI was a significant predictor of yield (R^2 ranged between 0.63 and 0.72) for a series of artificially eroded plots in central Missouri. Lindstrom et al. (1992) compared PI values estimated with the Soil Conservation Service (SCS) Soil Interpretation Record (SIR) database to PI values determined from field data measured by erosion class for selected soils in the Corn Belt. Correlation coefficients for the PI values calculated using the SIR data base and those calculated from the measured erosion data were reasonably good, R^2 was 0.72 for PI with 0 cm soil removed and 0.66 for PI with 50 cm soil removed. The discrepancies occurred because the input SIR database is derived from an average of many pedons across the locational range of a soil

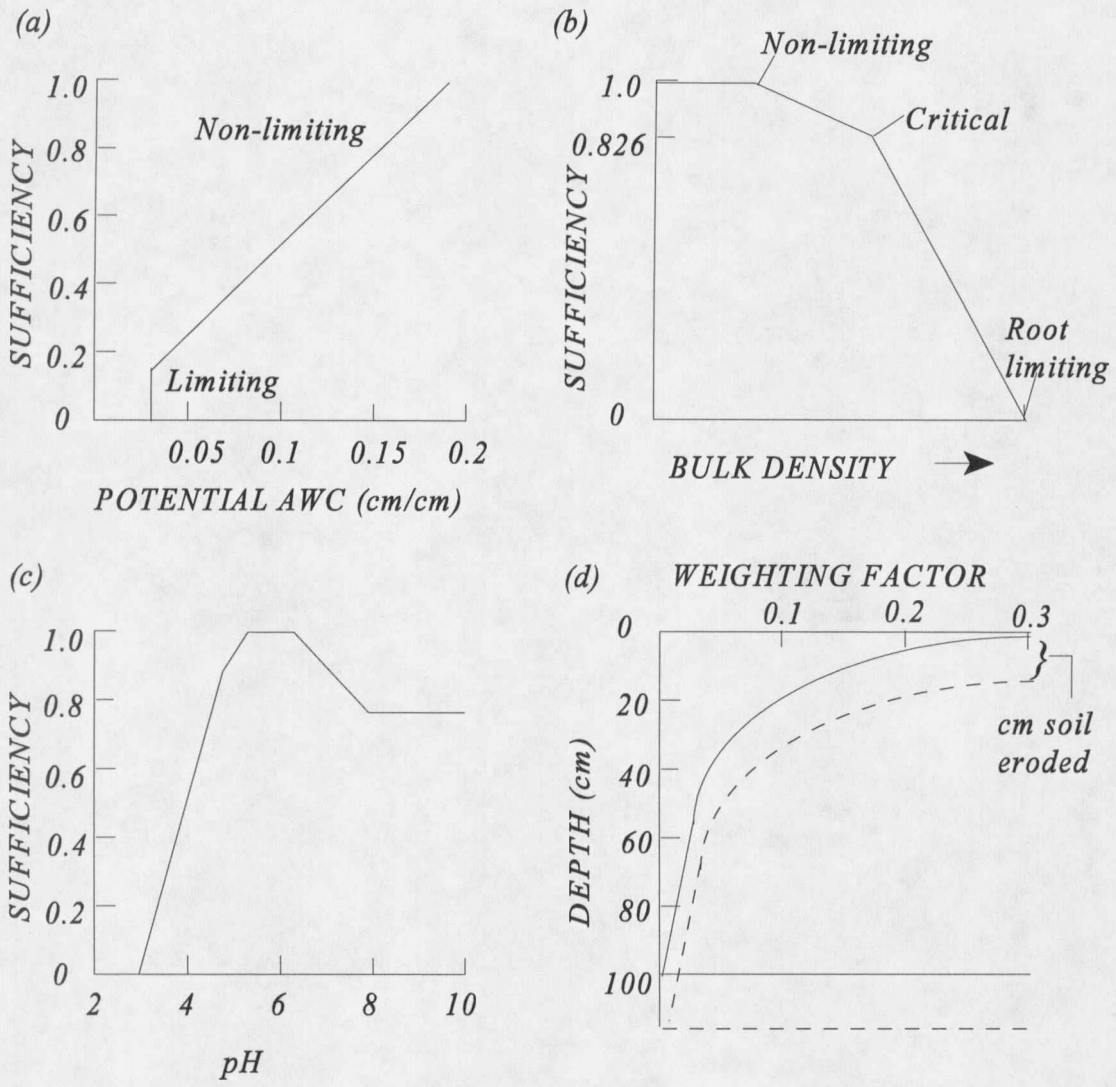

FIGURE 6. Sufficiencies of (a) potential available water capacity, (b) bulk density, (c) pH, and (d) concept of the sliding weighting factor used in the Productivity Index (PI) model. As erosion occurs, the curve shifts down the soil profile. PI drops if the subsoil has characteristics less favorable than the soil above it. If a limiting layer is encountered, that portion of the curve below the limiting layer is lost and PI declines. The solid line represents the assumed rooting pattern (weighting factor) for 100 cm depth in an ideal soil, (after Pierce et al., 1983). No units are reported on the X-axis in (b) because the non-limiting, critical, and root-limiting bulk densities vary with soil family texture class.

series, whereas the measured data were collected at specific sites. The results of these comparisons show that the PI model will characterize soil productivity at specific sites more precisely if accurate field data are available.

Modified versions of the PI model have been successfully applied to several locations outside the U.S. Corn Belt, including northern Great Plains small grain environments (Montana), and tropical regions (Nigeria, Hawaii, India, and Mexico). Wilson et al. (1991, 1992) used soils and crop data measured in the field as well as data extracted from the national SOILS-5 database (a predecessor to the SIR database referred to earlier) to evaluate PI model performance in Montana. Regressions of yield against PI produced R^2 values of 0.64, 0.67, 0.63 and 0.1 in four fields when the original PI was used. The mean R^2 in all four fields was increased by an average of 44 percent when the content and location of organic matter and $CaCO_3$ in the soil profile was considered, and an additional 9 percent (from 0.69 to 0.75) when cropping history was considered (Wilson et al., 1991). Regressions of barley, spring and winter wheat soil survey yield estimates against PI from the original model in Cascade County accounted for 34, 31 and 31 percent of the variability in yields of these three crops, respectively (Wilson et al., 1992). R^2 values increased an average of 77 percent and accounted for 54, 59 and 58 percent of the variations in yields when four new factors were added to the model to account for the effects of water balance, slope, growing degree days and calcium carbonate content (Wilson et al., 1992). However, potential problems affecting the yield data reported in county soil surveys may have prevented further improvements in model performance in the Cascade County application (Baker and Gersmehl, 1991; Brown,

1993; Gersmehl and Brown, 1986; Wilson et al., 1991). Rijsberman and Wolman (1985) compared PI model performance in several tropical locations (Nigeria, Hawaii, India, Mexico) and concluded that the PI approach is a promising tool so long as the model is modified to account for local soil characteristics. Soil penetrometer measures provided a better indicator of root extension than bulk density for Hawaiian soils. On Nigerian and Hawaiian soils, a factor relating crop response to organic carbon improved the performance of PI in describing productivity.

These results show how the PI model can be used for regional assessments of the crop productivity impacts of soil erosion. In addition, the original PI model requires fewer inputs compared to other simulation models (e.g., Williams et al., 1983). Pierce et al. (1984c) and Wilson et al. (1991, 1992) suggested adding a sufficiency factor to account for the adequacy of the growing season water supply to the PI model when it is applied to semi-arid landscapes. The current study used existing data for Montana to generate a sufficiency factor for growing season water supply (deficit) and to show how the revised model may be applied in semi-arid landscapes to evaluate the productivity effects of soil erosion and/or climate change.

METHODS AND DATA SOURCES

We chose a subset of soils from the State Soil Geographic Data Base (STATSGO; USDA-NRCS, 1994) with a large spatial coverage in Montana, assuming that a mapping unit is comprised of one particular soil. We predicted yields for those soils using a modified form of the current USDA-NRCS Montana yield model and GIS-based maps of

growing season precipitation and consumptive water use (potential evapotranspiration) as described in Chapter 2. We then overlaid the soil and climate grids, and calculated water deficit and yield for each grid cell. For each soil we extracted the corresponding yield-water deficit pairs and regressed them against each other. The results of the regression analysis were used to guide the development of a generic curve for growing season water supply (water deficit) sufficiency. Finally, the revised model was used to illustrate how the productivity impacts of soil erosion and/or climate change can be estimated with this modified PI model in semi-arid landscapes.

Growing Season Water Supply

Mean monthly precipitation grids for Montana were generated with ANUSPLIN (Hutchinson, 1989a, 1995, Custer et al., 1996). This model uses Laplacian thin plate smoothing splines with location (latitude, longitude) and elevation (in kilometers above sea level) to interpolate mean monthly minimum and maximum precipitation for the period 1961-90. Monthly data for 954 stations in Montana and parts of Alberta, Saskatchewan, North Dakota, South Dakota, Wyoming, and Idaho were used as inputs. Stations from adjacent provinces and states were included to account for edge effects and stations with longer records were weighted more heavily than stations with shorter or incomplete records. A growing season precipitation grid was produced by adding the mean monthly precipitation grids for May, June, and July.

The growing season potential evapotranspiration grid was calculated from mean monthly temperature and monthly percentage of annual daylight hours grids for Montana

using the Blaney -Criddle consumptive use method (Blaney and Criddle, 1950; USDA-SCS, 1988; 1993) implemented in the ARC/INFO GIS (Chapter 2). Spatially distributed growing season consumptive water use (CU) values were computed for Montana spring wheat as follows:

$$CU = K \sum_{i=1}^{3} p_i \, t_i \, / \, 100 \qquad (3)$$

where K is an empirical consumptive water use crop coefficient for the growing season, p_i is the monthly percentage of annual daylight hours, t_i is the mean monthly air temperature in degrees Fahrenheit, and $i = 1, 2, 3$ for May, June, July (i.e., the growing season for spring grain in Montana). Consumptive water use crop coefficients have been determined experimentally at numerous localities for most crops grown in the western U.S. For small grains with a three month growing season the empirical consumptive water use crop coefficient for the growing season (K) equals 0.75 for more humid and 0.85 for more arid areas (USDA-SCS, 1993). The latter value was used in this study. The mean monthly temperature grids were generated with the same ANUSPLIN interpolation program as were the precipitation grids. The monthly percentage of annual daylight hours (p_i) grids were generated from ASCII files containing interpolated p-values for each growing season month for the latitudes of the grid cell midpoints. Original p-values were taken from the National Engineering Handbook (USDA-SCS, 1993) and p-values for the intermediate latitudes were interpolated as described in Chapter 2.

Water deficit values were obtained for each soil series. For each soil series we

extracted the mapping units containing the particular soil from the STATSGO data base as an ARC/INFO coverage of that soil assuming that the entire mapping unit was comprised of that particular soil. This coverage was converted into a grid (as described in the next section) and overlaid with the growing season precipitation and consumptive water use grids. The water deficit (D) was estimated as the difference between consumptive water use (which is equivalent to potential evapotranspiration) and growing season precipitation (GSP):

$$D = CU - GSP \tag{4}$$

In this way, spatially distributed water deficit values were calculated only for those cells where the particular soil could have occurred.

Yield Predictions

To obtain spatially distributed continuous yield estimates for each soil series we used the USDA-NRCS Montana yield model as summarized in Chapter 2:

$$Yield = IYP + GYC\ (GSP + AWC + adjustments) \tag{5}$$

where IYP is the initial yield point, GYC is a grain yield coefficient, GSP is the growing season precipitation in inches, and AWC is the potential water holding capacity of the soil in inches. Both the GYP and IYP inputs vary with the choice of crop and consumptive water use area (Brown and Carlson, 1990). Adjustments (in inches) are made for slope, soil particle size, water table depth, ponding, organic matter content, lime content, and

sodium content. TABLE 8 shows the equations for spring wheat and the four consumptive water use areas developed by Brown and Carlson (1990).

TABLE 8. Yield equations for spring wheat developed by Brown and Carlson (1990) and used in the Montana Yield Model (USDA-NRCS).

Consumptive use area	Yield equation for spring wheat
1	Yield = 4.7 * (GSP + AWC + adjustments) - 3.8
2	Yield = 5.1 * (GSP + AWC + adjustments) - 3.8
3	Yield = 5.8 * (GSP + AWC + adjustments) - 3.8
4	Yield = 6.1 * (GSP + AWC + adjustments) - 3.8

These equations predict higher yields in areas of lower consumptive use since plants in areas of high consumptive water use will be subjected to a greater water stress (Brown and Carlson, 1990). Because the model calculates yield for each soil using up to four different equations (i.e., one for each of the consumptive water use zones; TABLE 8), an artificial division of yield values by consumptive water use zone was introduced. This split in yield values is reflected in the yield - water deficit scatterplots (FIGURE 7). The split is artificial because the spatial pattern of those consumptive water use zones is questionable. However, we treated the yield values as a continuum and used them as is because they represented the best yield data available for the state of Montana at this time.

The *AWC* and related adjustments used in Equation 4 were obtained from the STATSGO database (USDA-NRCS, 1994). For each soil series we added the mean of the minimum and maximum *AWC* values to the calculated adjustments and attached this sum

to the attribute table of the appropriate soil coverage. The coverage was then converted into a grid using the adjusted soil water availability as grid values. The adjusted soil water availability grid for each soil series was combined with the growing season precipitation (*GSP*) and consumptive water use (*CU*) grids. The consumptive water use information was used to assign grid cells into consumptive water use zones 1 through 4, and the appropriate yield equation was applied to estimate yields for each subset of grid cells. The water deficit and yield information for each soil series was then combined in a single attribute table.

In this study we used existing data for Montana. These data were not collected in the field but modeled in the ways described above. Growing season precipitation served as an input variable in the calculation of both yield and water deficit in our data modeling process. However, this may not be a concern since we are not interested in validating a cause-and-effect model, but in the shape of the curve describing the relationship between yield and growing season water supply. Besides, it is generally known that precipitation is a variable influencing both yield and growing season water supply, and the available water holding capacity was also used in both the yield and PI models. This circularity may not be important given the goal of this paper to generate a sufficiency curve for growing season water supply that might be used in semi-arid landscapes.

Regression Analysis (Model fitting)

To generate a sufficiency curve for water deficit we had to develop a general model fitting the yield and growing season water supply data. We displayed the data in

scatterplots showing growing season water supply (deficit) on the X-axis and yield on the Y-axis. As expected, yield values decrease with increasing water deficit. The relationship between yield and water deficit was linear for each of the chosen soils. Therefore, we used linear regression to describe the shape of the data cloud. For the regression analysis, we created a yield and water deficit grid for each soil series. Regression can be performed in the ARC/INFO GRID module, but the output statistics do not include R^2 values (Version 7.1.1; ESRI, Inc., 1997a). We instead used the sample file function in the GRID module to generate sample files containing the corresponding yield - water deficit data pairs and the geographic coordinates for all grid cells covered by a particular soil series. The regressions were then performed with the General Linear Model procedure in SAS (Version 6.12; SAS Institute, Inc., 1997).

A general yield - water deficit model was created where the intercept is the mean of the soil-specific regression intercepts and the slope is the mean of the soil-specific regression slopes for soils with $R^2 > 0.7$. This general model was then normalized to produce a sufficiency curve where a water deficit of 0 corresponds to a sufficiency of 1 and the deficit value for which yield is 0 corresponds to a sufficiency of 0. The water deficit was converted from inches into centimeters prior to normalization because the original PI model used metric units. This sufficiency of growing season water supply was then added as a factor in the PI model. Soil erosion and/or climate change or fluctuation were then simulated using the modified PI model to illustrate their impact on productivity. Maps showing the spatial distribution of the corresponding modified PI estimates for the Cherry silt loam series on 2-8 percent slopes were produced using the

ArcView GIS (Version 3.0a, ESRI, 1997b). Spatial analyses of percent change in PI were also performed in the ArcView GIS.

RESULTS AND DISCUSSION

By examining multiple occurrences of the same soil series across Montana we held all factors but climate constant. This approach meant that we could explore the effect of water supply (deficit) on yields in isolation of other influences. TABLE 9 summarizes the results of our regression analysis. All regression models have similar shapes (forms) with a large intercept and a negative slope. The negative slope indicates that predicted yield decreases with increasing water deficit (FIGURE 7). The three different symbols in FIGURE 7 show the artificial discontinuities in the yield values noted earlier.

TABLE 9. Regression results of water deficit in inches versus yield in bushels per acre ordered by decreasing R^2.

Soil Series Name	Slope Range in %	Surface Texture Class[1]	Sample Size n	Regression Intercept	Regression Slope	R^2
Slocum	0-4	L	387	109.22	-5.66	0.99
Cherry	2-8	SIL	5273	112.72	-5.76	0.93
Adel	4-15	L	915	113.50	-5.89	0.92
Delpoint	8-15	L	24892	104.31	-5.33	0.91
Musselshell	2-8	L	3376	94.05	-4.65	0.90
Gerdrum	0-8	CL	26222	96.74	-4.73	0.90
Korchea	0-4	L	8254	117.25	-6.14	0.89
Cabbart	2-15	L	8648	105.59	-5.48	0.87

Soil Series Name	Slope Range in %	Surface Texture Class[1]	Sample Size n	Regression Intercept	Regression Slope	R^2
Busby	2-15	FSL	16726	82.84	-4.05	0.87
Gerdrum	2-8	CL	21816	97.82	-4.84	0.85
Hillon	4-15	CL	34379	98.51	-5.33	0.85
Cabba	8-35	L	8979	84.93	-4.87	0.83
Yamac	2-8	L	40322	103.68	-5.01	0.82
Havre	0-2	L	62592	99.43	-4.59	0.82
Delpoint	2-15	L	6980	103.45	-5.20	0.82
Neldore	2-15	CL	6554	96.14	-5.14	0.81
Twilight	2-15	FSL	18832	89.49	-4.60	0.81
Havre	0-4	L	59581	110.68	-5.67	0.78
Ryell	0-2	L	4013	108.19	-5.36	0.78
Ethridge	0-4	SICL	14114	121.95	-6.22	0.77
Harlem	0-2	SICL	10601	105.15	-5.41	0.77
Havrelon	0-4	SIL	14062	87.84	-3.46	0.76
Kobar	0-8	SICL	28581	108.34	-5.42	0.75
Harlem	0-2	SIC	17850	94.37	-4.48	0.75
Yamac	2-15	L	11382	101.48	-5.03	0.74
Scobey	0-8	CL	26803	114.66	-5.71	0.73
Yawdim	4-15	SICL	7571	105.28	-5.64	0.73
Shambo	0-4	L	16787	110.70	-5.25	0.72
Lambert	2-15	SIL	19181	90.49	-3.53	0.71
Scobey	0-4	CL	27158	117.32	-6.01	0.70
Trembles	0-4	FSL	12279	79.04	-3.44	0.61
Glendive	0-2	SL	4787	105.37	-6.08	0.61

Soil Series Name	Slope Range in %	Surface Texture Class[1]	Sample Size n	Regression Intercept	Regression Slope	R^2
Trembles	0-2	FSL	19402	78.59	-3.40	0.51
Glendive	0-2	FSL	5076	61.49	-2.05	0.16
Havrelon	0-2	SIL	4913	65.87	-1.24	0.04

[1] CL = clay loam, FSL = fine sandy loam, L = loam, SIC = silty clay, SICL = silty clay loam, SIL = silty loam, and SL = sandy loam surface textures.

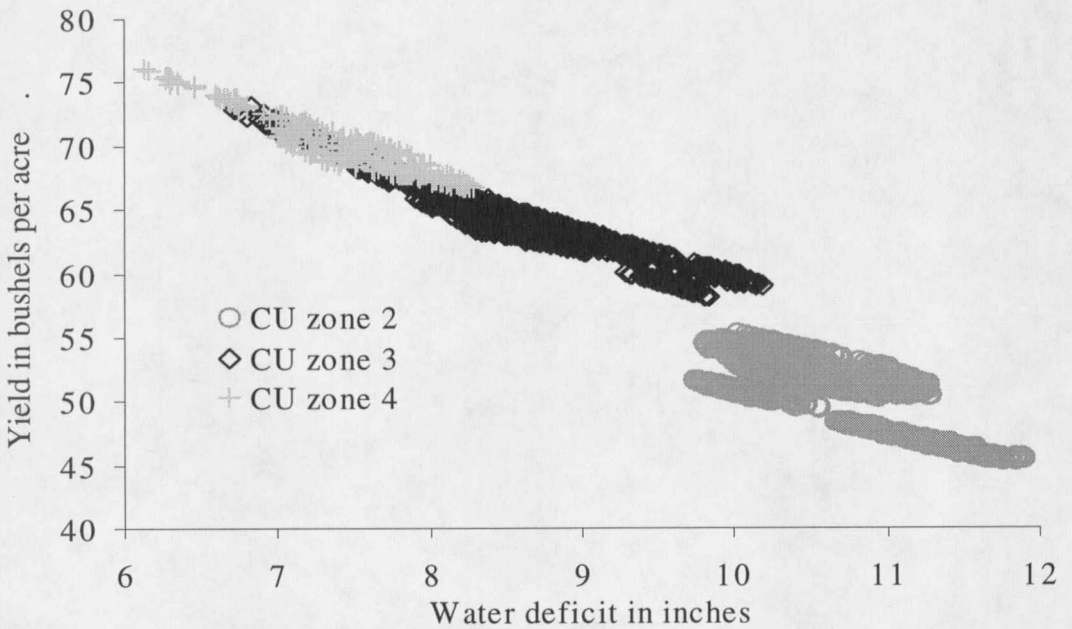

FIGURE 7: Yield-water deficit scatterplot for Cherry silt loam on 2-8 percent slopes, (n = 4,920).

FIGURE 8 shows that the water deficit explained at least 70 percent of the variability in yield for 30 of 35 soils examined in this study. This result is not unexpected given the ways in which we held other contributing factors constant and calculated (estimated) yields. FIGURE 8 also shows a breakpoint in R^2 values at 0.7. Soils with the low R^2

values < 0.7 were characterized by either fine sandy loam surface textures on slopes between 0-4 percent, sandy loam surface textures on 0-2 percent slopes, or silt loam surface textures on 0-2 percent slopes. This result suggests a pattern in the soils themselves since these surface texture - slope range combinations were not encountered among the soils with higher R^2 values. However, there was also some evidence that the soils with R^2 values < 0.77 are concentrated in high consumptive water use areas (i.e., CU classes 1, 2, and 3) compared to soils with higher R^2 values (CU classes 2, 3, 4, and 5). This pattern may indicate that the yield model performs better in low consumptive water us areas.

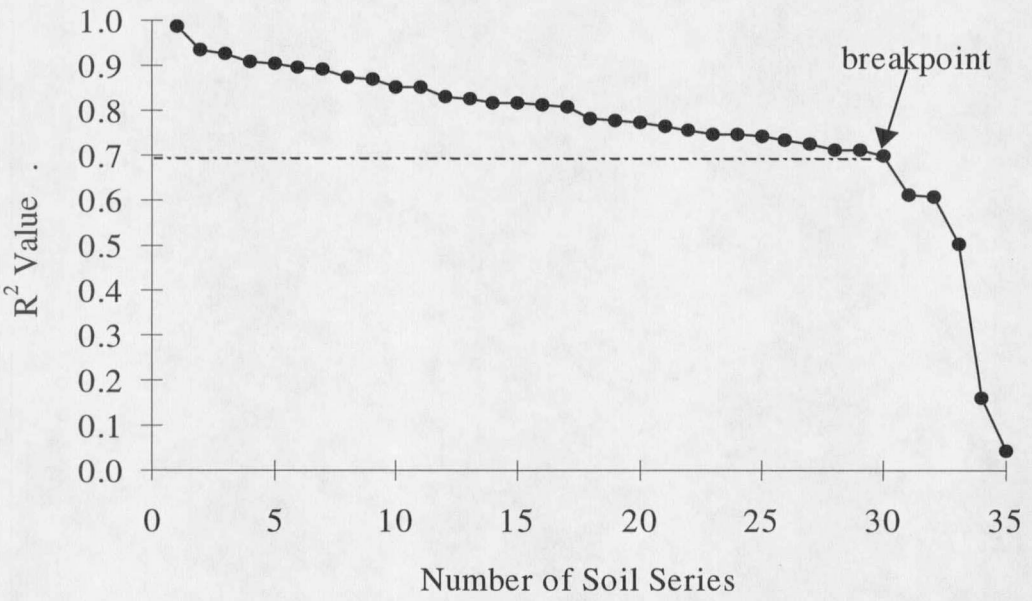

FIGURE 8: Plot of R^2 values in descending order.

These regression results were used to prepare a generalized growing season water supply sufficiency curve similar to those used for pH, AWC, and BD in the original PI model (FIGURE 9). The mean regression intercepts and slopes were calculated over the first 30 soils in TABLE 9 for which $R^2 > 0.7$, such that:

$$Yield\ (in\ bushels\ per\ acre) = 102.87 - 5.149\ Deficit\ (in\ inches) \quad \textbf{(6)}$$

The growing season water supply sufficiency curve derived from the general model after water deficit was converted to centimeters has the form:

$$WS_{suff} = 1 - 0.0197\ WD \quad \textbf{(7)}$$

where WS_{suff} is the dimensionless growing season water supply sufficiency ($0 \leq WS_{suff} \leq 1.0$), and D is water deficit in centimeters. The solid line in FIGURE 9 represents the part of the sufficiency curve that can be filled by Montana data (TABLE 10), and we have sketched in a gray dotted line at either end to match the idealized S-curve proposed by Pierce et al. (1984c).

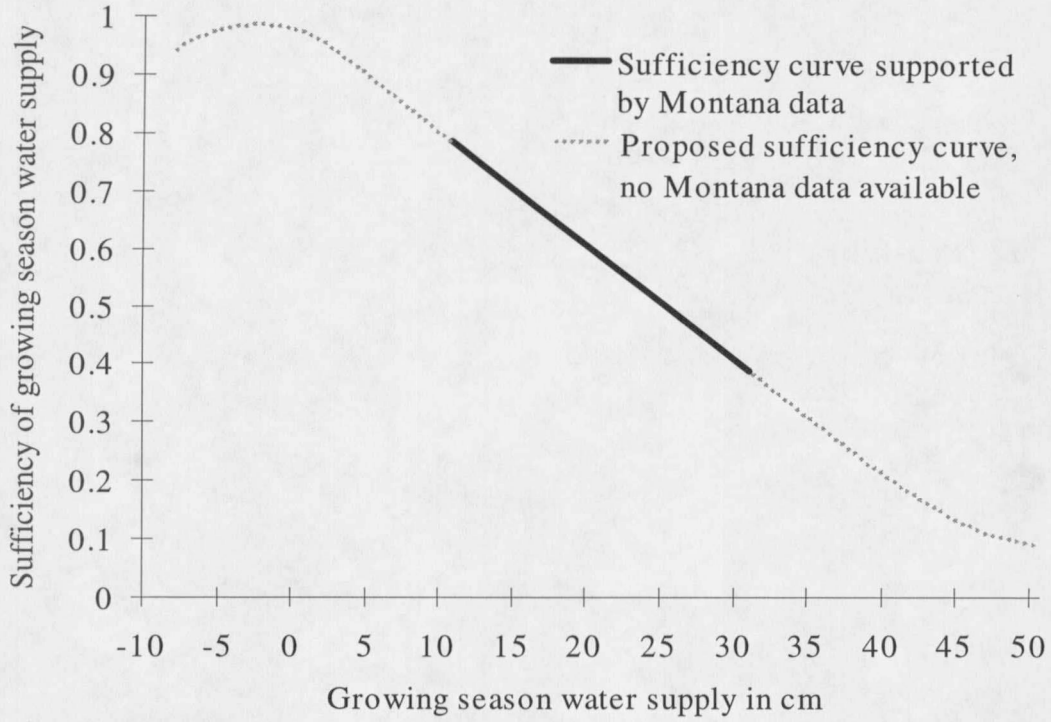

FIGURE 9: Sufficiency of growing season water supply plotted against growing season water supply in centimeters.

TABLE 10. Predicted water deficits and water supply sufficiencies for the soils used in the sufficiency curve generation process.

Soil Name	Slope Range in %	Surface Texture Class[1]	Max. Water Deficit in mm	Min. Water Deficit in mm	Min. Water Supply Sufficiency	Max. Water Supply Sufficiency
Slocum	0-4	L	283	120	0.443	0.764
Cherry	2-8	SIL	302	125	0.405	0.754
Adel	4-15	L	266	140	0.477	0.724
Delpoint	8-15	L	309	135	0.392	0.735
Musselshell	2-8	L	303	146	0.403	0.713

Soil Name	Slope Range in %	Surface Texture Class[1]	Max. Water Deficit in mm	Min. Water Deficit in mm	Min. Water Supply Sufficiency	Max. Water Supply Sufficiency
Gerdrum	0-8	CL	302	126	0.405	0.752
Korchea	0-4	L	293	108	0.423	0.786
Cabbart	2-15	L	293	109	0.422	0.786
Busby	2-15	FSL	310	216	0.390	0.575
Gerdrum	2-8	CL	302	183	0.405	0.640
Hillon	4-15	CL	309	199	0.392	0.609
Cabba	8-35	L	284	125	0.440	0.754
Yamac	2-8	L	303	194	0.403	0.619
Havre	0-2	L	310	134	0.390	0.736
Delpoint	2-15	L	310	178	0.390	0.649
Neldore	2-15	CL	298	208	0.412	0.591
Twilight	2-15	FSL	301	206	0.407	0.594
Havre	0-4	L	309	188	0.392	0.630
Ryell	0-2	L	303	134	0.403	0.736
Ethridge	0-4	SICL	304	199	0.402	0.608
Harlem	0-2	SICL	305	172	0.399	0.662
Havrelon	0-4	SIL	302	237	0.406	0.533
Kobar	0-8	SICL	308	167	0.393	0.670
Harlem	0-2	SIC	305	182	0.399	0.641
Yamac	2-15	L	310	193	0.390	0.620
Scobey	0-8	CL	308	199	0.393	0.609
Yawdim	4-15	SICL	310	193	0.390	0.620
Shambo	0-4	L	301	182	0.407	0.641

Soil Name	Slope Range in %	Surface Texture Class[1]	Max. Water Deficit in mm	Min. Water Deficit in mm	Min. Water Supply Sufficiency	Max. Water Supply Sufficiency
Lambert	2-15	SIL	302	236	0.405	0.534
Scobey	0-4	CL	302	204	0.406	0.598

1 See notes at end of TABLE 9 for description of surface texture class codes.

The sufficiency of growing season water supply (WS_{suff}) was then added as another factor in the PI model:

$$PI = WS_{suff} \sum_{i=1}^{n} A_i \, C_i \, D_i \, WF_i \qquad (8)$$

We would expect lower PI values in semi-arid landscapes given: (1) the PI model approach of multiplying sufficiencies ranging between 0 and 1, and (2) the knowledge that the growing season water supply sufficiency in Montana is almost always less than 1.0 (solid line in FIGURE 9).

The PI model was initially proposed as a way to determine the vulnerability of soils to productivity losses caused by erosion (soil removal) (Pierce et al., 1983, 1984a, 1984b). We applied this new PI model to the 30 Montana soils used for model development to evaluate their vulnerability to soil loss. In addition, we examined the sensitivity of the productivity of these soils to change in water deficit (climate change) as expressed in PI.

TABLE 11 summarizes the results of original PI model runs (Equation 2; TABLE 11, column 5) compared to runs with the modified model (Equation 8;

TABLE 11, columns 6-9) for these 30 Montana soils and the percent change in PI under the specified conditions of soil removal and water deficit increase (TABLE 11, columns 10-12). The S5ID (column 4) was used to integrate soil mapping units and the AWC, pH, bulk density, and permeability per soil layer per soil series. The average modified PI (column 6) is the mean of the minimum and maximum modified PI that resulted from the minimum and maximum sufficiencies in water supply for each soil (TABLE 10). As expected, the modified PI is smaller than the original PI. The removal of 10 cm of soil resulted in a 0-25 percent change in the modified PI (6 percent change on average). A change of this magnitude would occur over many decades since the usual soil erosion threshold of 12 metric t/ha/yr is equal to the removal of approximately 1 cm of soil per decade. Soils with a high vulnerability to soil loss (largest change in modified PI) are usually thin soils such as the Cabba, Cabbart, Neldore, and Yawdim series. In contrast, an increase in water deficit of 10 cm produced changes of 33-42 percent in the modified PI (36 percent change on average). This result indicates that the productivity is very sensitive to a 10 cm change in water supply in semi-arid landscapes like those found in Montana.

TABLE 11. Results of PI model runs for 30 Montana soils.

Soil Series Name	Slope Range in %	Surface Texture Class[1]	S5ID	PI original	Average PI modified	Average modified PI with			Percent change from the average modified PI to the average modified PI with		
						10 cm soil removed	10 cm increase in water deficit	10 cm soil removed and 10 cm increase in water deficit	10 cm soil removed	10 cm increase in water deficit	10 cm soil removed and 10 cm increase in water deficit
ADEL	4-15	L	MT0075	0.897	0.539	0.528	0.362	0.355	1.9	32.8	34.1
			MT0831	0.81	0.486	0.462	0.327	0.311			36.1
BUSBY	2-15	FSL	MT0167	0.597	0.288	0.285	0.170	0.168	1.2	40.8	41.5
CABBA	8-35	L	MT0048	0.361	0.215	0.161	0.144	0.108	25.2	33.0	49.9
CABBART	2-15	L	MT0050	0.498	0.301	0.254	0.203	0.171	15.7	32.6	43.2
CHERRY	2-8	SIL	ND0283	0.733	0.425	0.417	0.280	0.275	1.8	34.0	35.2
			ND0331	0.757	0.439	0.435	0.289	0.287			34.6
DELPOINT	2-15	L	MT0271	0.604	0.314	0.275	0.195	0.171	12.3	37.9	45.5
DELPOINT	8-15	L	MT0271	0.604	0.340	0.299	0.221	0.194	12.3	35.0	42.9
ETHRIDGE	0-4	SICL	MT0093	0.773	0.390	0.359	0.238	0.219	8.2	39.0	44.0

Soil Series Name	Slope Range in %	Surface Texture Class[1]	S5ID	PI original	Average PI modified	Average modified PI with			Percent change from the average modified PI to the average modified PI with		
						10 cm soil removed	10 cm increase in water deficit	10 cm soil removed and 10 cm increase in water deficit	10 cm soil removed	10 cm increase in water deficit	10 cm soil removed and 10 cm increase in water deficit
GERDRUM	0-8	CL	MT0286	0.359	0.208	0.185	0.137	0.122	10.9	34.1	41.2
GERDRUM	2-8	CL	MT0286	0.359	0.188	0.167	0.117	0.104	10.9	37.7	44.5
HARLEM	0-2	SIC	MT0101	0.721	0.375	0.374	0.233	0.232	0.1	37.9	38.0
			MT0186	0.612	0.318	0.317	0.197	0.197			38.1
			MT0187	0.616	0.320	0.317	0.199	0.197			38.5
			MT0232	0.401	0.208	0.192	0.129	0.119			42.7
			MT1008	0.463	0.241	0.229	0.149	0.142			41.0
HARLEM	0-2	SICL	MT0101	0.76	0.403	0.398	0.253	0.250	1.3	37.2	38.0
			MT0186	0.623	0.330	0.323	0.208	0.203			38.5
			MT0187	0.619	0.328	0.323	0.206	0.203			38.1
			MT0232	0.45	0.239	0.212	0.150	0.133			44.1
			MT0863	0.642	0.340	0.313	0.214	0.197			42.2
HILLON	4-15	CL	MT0103	0.744	0.372	0.372	0.226	0.226	0.0	39.4	39.4

Soil Series Name	Slope Range in %	Surface Texture Class[1]	S5ID	PI original	Average PI modified	Average modified PI with			Percent change from the average modified PI to the average modified PI with		
						10 cm soil removed	10 cm increase in water deficit	10 cm soil removed and 10 cm increase in water deficit	10 cm soil removed	10 cm increase in water deficit	10 cm soil removed and 10 cm increase in water deficit
HAVRELON	0-4	SIL	ND0297	0.834	0.391	0.389	0.227	0.226	0.5	42.0	42.3
HAVRE	0-2	L	MT0072	0.729	0.410	0.399	0.267	0.260	2.6	35.0	36.7
			MT0181	0.471	0.265	0.265	0.172	0.172	0.0	35.0	35.0
			MT0188	0.755	0.425	0.416	0.276	0.271	2.0	35.0	36.3
			MT0744	0.729	0.410	0.399	0.267	0.260	2.6	35.0	36.7
			MT0745	same				0.260			
			MT0773	0.783	0.441	0.433	0.286	0.282	1.7	35.0	36.1
HAVRE	0-4	L	MT0072	0.729	0.372	0.363	0.229	0.223	2.6	38.6	40.2
			MT0181	0.471	0.241	0.241	0.148	0.148	0.0	38.6	38.6
			MT0188	0.755	0.386	0.378	0.237	0.232	2.0	38.6	39.8
			MT0744	0.729	0.372	0.363	0.229	0.223	2.6	38.6	40.2
			MT0745	same							
			MT0773	0.783	0.400	0.393	0.246	0.242	1.7	38.6	39.6
KOBAR	0-8	SICL	MT0106	0.717	0.381	0.367	0.240	0.231	3.8	37.1	39.4

Soil Series Name	Slope Range in %	Surface Texture Class[1]	S5ID	PI original	Average PI modified	Average modified PI with			Percent change from the average modified PI to the average modified PI with		
						10 cm soil removed	10 cm increase in water deficit	10 cm soil removed and 10 cm increase in water deficit	10 cm soil removed	10 cm increase in water deficit	10 cm soil removed and 10 cm increase in water deficit
KORCHEA	0-4	L	ND0260 ND0300	0.748 same	0.452	0.441	0.305	0.297	2.4	32.6	34.2
LAMBERT	2-15	SIL	MT0011	0.869	0.408	0.404	0.237	0.234	1.0	42.0	42.6
MUSSEL-SHELL	2-8	L	MT0442	0.621	0.347	0.324	0.224	0.209	6.6	35.3	39.6
NELDORE	2-15	C	MT0347	0.396	0.199	0.166	0.121	0.101	16.7	39.3	49.4
RYELL	0-2	L	MT0208	0.65	0.370	0.336	0.242	0.220	9.2	34.6	40.6
			MT0877 MT0678	0.478	0.272	0.233	0.178	0.153	14.2	34.6	43.9
SCOBEY	0-4	CL	MT0124	0.456	0.229	0.186	0.139	0.113	18.9	39.3	50.7
SCOBEY	0-8	CL	MT0124	0.456	0.228	0.185	0.138	0.112	18.9	39.4	50.8

Soil Series Name	Slope Range in %	Surface Texture Class[1]	S5ID	PI original	Average PI modified	Average modified PI with			Percent change from the average modified PI to the average modified PI with		
						10 cm soil removed	10 cm increase in water deficit	10 cm soil removed and 10 cm increase in water deficit	10 cm soil removed	10 cm increase in water deficit	10 cm soil removed and 10 cm increase in water deficit
SHAMBO	0-4	L	ND0257	0.838	0.439	0.424	0.274	0.265	3.3	37.6	39.7
SLOCUM	0-4	L	MT0245	0.791	0.477	0.464	0.321	0.313	2.7	32.7	34.4
TWILIGHT	2-15	FSL	SD0395	0.549	0.275	0.245	0.167	0.149	10.7	39.4	45.9
YAMAC	2-15	L	MT0138	0.707	0.357	0.343	0.217	0.209	3.8	39.0	41.4
YAMAC	2-8	L	MT0138	0.707	0.361	0.347	0.222	0.213	3.8	38.6	40.9
YAWDIM	4-15	SICL	ND0262	0.434	0.219	0.177	0.134	0.108	19.4	39.0	50.8

[1] See notes at end of TABLE 9 for description of surface texture class codes.

We also examined the combined effect of climate change or fluctuation and soil erosion losses (TABLE 11, columns 9 and 12). The removal of 10 cm of soil in combination with an increase of 10 cm in water deficit produced the largest change in modified PI, namely between 34 and 51 percent (an average of 41 percent change).

FIGURE 10 shows the spatial distribution of the modified productivity index values for Cherry silt loam on 2-8 percent slopes in Montana. Higher PI values were estimated in the southern STATSGO soil mapping units containing the Cherry soil series and lower PI values in the northern map units. A similar gradient is evident as one moves from the western to the eastern map units. The maps illustrate that the spatial coverage of lower modified PI values is larger than the spatial coverage of higher estimates. This is also reflected in the low value of the spatially weighted average modified PI (0.379) which is close to the low end of the range of modified PI estimates (0.307-0.536). These maps also show that the variability of PI values within the southwestern Cherry soil area is higher than the variability within the eastern and northern areas. This is a reflection of the mountainous landscape where evapotranspiration varies more (over short distances) than on the Great Plains (eastern Montana). However, it is important to remember that in using the STATSGO database we assumed that each of these STATSGO mapping units consisted of the one soil although a mapping unit may contain up to 21 different soils (Reybold and TeSelle, 1989; USDA-NRCS, 1994). In some areas where the maps show Cherry soil, Cherry soil series may not exist in reality and the variability may be much smaller.

FIGURE 10. Spatial distribution of modified PI for Cherry silt loam on 2-8 percent slopes.

FIGURE 11 shows changes in modified PI for the south-western mapping units of the Cherry silt loam series on 2-8 percent slopes under each of the following scenarios: (1) no change in soil erosion or water deficit (FIGURE 11a); (2) soil erosion has removed 10 cm of soil (FIGURE 11b); (3) water deficit increased by 10 cm (FIGURE 11c); and (4) 10 cm of soil are eroded and water deficit increased by 10 cm (FIGURE 11d). For all four simulations the lowest PI values are seen in the south and/or east of those mapping units, the higher PI values are found in the north and north-west of the depicted areas. We computed the percentage of the total area covered by Cherry silt loam on 2-8 percent slopes for modified PI estimates that were less than some threshold value for the four simulations for Montana. We chose a threshold value of 0.3 arbitrarily as an example (assuming that below that productivity value crop production is impossible or non-profitable). While the modified PI estimates for simulations (1) and (2) for the entire area covered by Cherry silt loam are larger than 0.3, 88 percent of the total area are smaller than 0.3 for simulations (3) and (4). For the Cherry soil areas represented in FIGURE 11, the results imply that for simulations (3) and (4) all of the eastern area and the eastern half of the western area could not be used for (profitable) crop production (FIGURES 11c and 11d). Maps indicating such non-profitable/unproductive areas can be produced for each soil series. Additionally, we computed that the spatially weighted modified PI decreases by 2 percent when 10 cm soil is eroded and by 38 percent when water deficit is increased by 10 cm, for the entire Cherry soil grid. These results are similar to the non-spatial average changes in TABLE 11 (2 and 34 percent decreases in productivity, respectively, for Cherry silt loam). The maps in FIGURE 11 illustrate how the impacts of erosion

and/or climate fluctuation are likely to vary spatially.

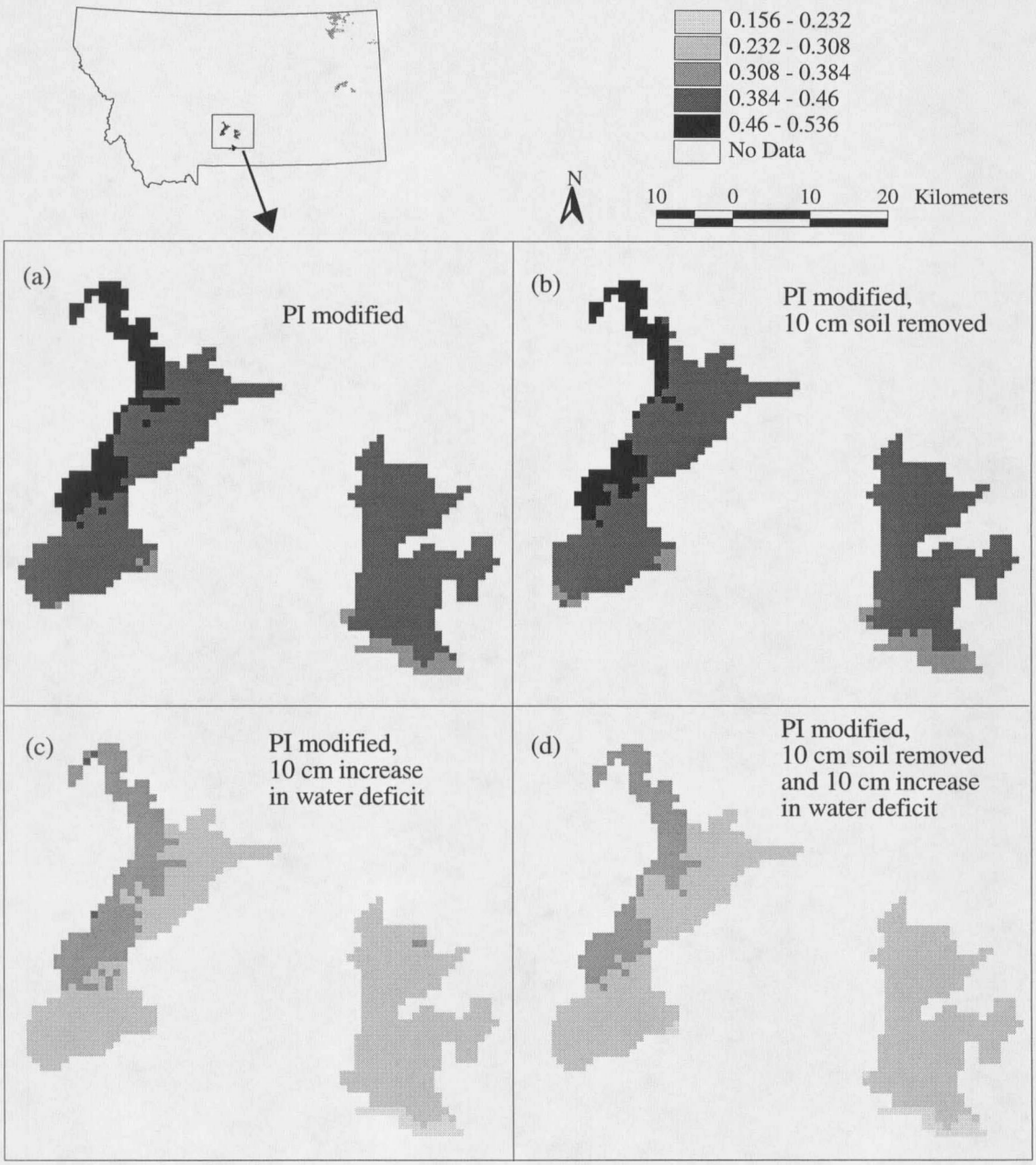

FIGURE 11. Spatial change in modified PI values for the south-western mapping units of the Cherry silt loam series on 2-8 percent slopes under four different scenarios.

CONCLUSIONS

The type of model developed in this study is suited as a reconnaissance tool in semi-arid regions, especially in the developing world where data availability is a problem. This particular model has very modest data needs and a relatively simple conceptual basis (curves) and could be implemented easily in several GIS (Grid module of ARC/INFO, IDRISI , ARCVIEW Spatial Analyst Extension, GRASS, etc.). This offers advantages in terms of data (existing data could be used, e.g., topographic and climate database for Africa (Hutchinson et al., 1996)), ease of use (AML, AVENUE programs, etc.), and clarity of output. Maps can be produced showing areas that are more/less vulnerable to productivity losses caused by climate change and/or accelerated erosion. The coarse data used in the current study did not contain detailed enough spatial information to display all of the agricultural soils of Montana in one map, and limits applications to region and state-wide analysis. We used the STATSGO soil database for the state of Montana in the current study because it provides the only spatial digital soil data that is currently available for the state. The STATSGO database is used primarily for river basin, multi-state, state, and multi-county resource planning, management, and monitoring (Mausbach et al., 1989; Reybold and TeSelle, 1989). STATSGO was created by generalizing detailed soil surveys and similar information. One mapping unit usually covers a large area and may contain up to 21 components (soil series).

Digital copies of the SSURGO database should be available for the state of Montana in about 2008 (Connie Williams, USDA-NRCS State Office, personal

communication, 1997). SSURGO is used primarily for farm and ranch conservation planning, range and timber management, and county and parish, township, and watershed resource planning and management (Mausbach et al., 1989; Reybold and TeSelle, 1989). One mapping unit may contain up to three components (soil series). With this more detailed data, the spatial extent of each soil can be determined more precisely. We had to assume that the entire mapping unit in the STATSGO database contains one particular soil. With the finer data water deficit values may be confined to a different range of values and the sufficiency of water supply may be recalculated to generate more specific PI values. These PI values may indicate the areas that are most vulnerable to productivity losses or alternatively they might be used to identify areas where more detailed analysis needs to be performed.

CHAPTER 4

SUMMARY AND CONCLUSIONS

The above research was undertaken to modify an existing measure of soil productivity requiring fewer inputs than other simulation models for use in semi-arid landscapes. The PI model developed by Pierce et al. (1983) for soils in the U.S. Corn Belt is one of the simplest and yet most successful approaches to quantify the relationship between soil erosion and soil productivity. We developed a sufficiency curve for growing season water supply that can be applied to semi-arid landscapes and added this sufficiency as a factor to the original PI model. Additionally, we illustrated impacts of (simulated) soil erosion and/or climate change or fluctuation on productivity. These results were accomplished using a series of GIS procedures with existing STATSGO, DEM, and climate data to minimize data collection and increase computational efficiency. GIS served as an efficient tool to: (1) estimate the necessary spatial data for Montana such as potential evapotranspiration, growing season precipitation, water deficit, and yield, (2) construct a more detailed consumptive water use map, and (3) display results.

The current study was divided into two parts where the results of the first part were integrated into the second. In the first part, problems inherent in the yield tables published in modern soil survey reports in the U.S. and the origins of the Montana Yield

Model were reviewed. Recent soil survey applications of the Montana Yield Model incorporate very detailed soil inputs and very generalized climatological inputs. The consumptive water use map used in this model exemplifies many of the map products that were produced prior to the widespread adoption and use of GIS and related geographic information technologies. We used the ANUSPLIN interpolation techniques with climate station records, digital elevation model data, and the ARC/INFO GIS to produce a series of new improved consumptive water use maps. These maps or data layers predicted noticeably different spatial and statistical patterns and magnitudes of consumptive water use across Montana compared with the original USDA-SCS map. For all comparison analyses the best agreement was found among the polygons which belonged to classes of low consumptive water use (mountainous areas) in both the GIS-based and original USDA-SCS maps. The percent agreement between the two maps was less than 50 percent in 20 of the 22 polygons assigned to classes of higher consumptive water use (agriculturally important areas). A map of the spatial pattern of the percent agreement per polygon for the CU overlay illustrates low agreement in most of the dryland farming areas and higher agreement in non-arable areas. These results have important implications for the Montana Yield Model because the polygons of low agreement incorporate the major crop producing areas in the state. Inaccurate polygon delineation and therefore class assignment may have a substantial impact on the accuracy of the model's yield predictions.

The larger number of climate stations and DEM grid points coupled with the interpolation methods that were used to generate these estimates suggests that our new

maps provide a superior description of consumptive water use across the state of Montana. The GIS methods offer at least five additional advantages. First, the GIS-based maps provide spatially distributed estimates of potential evapotranspiration that allow the user to perform the final classification. Second, the GIS method can be used to produce temporal series of consumptive water use maps that provide monthly estimates of potential evapotranspiration and account for varying growing season lengths of different crops. Third, evapotranspiration was estimated at a finer spatial resolution than in the original USDA-SCS map. Data can be generated for different resolutions, either by aggregating to the required resolution or by specifying the desired cell size when interpolating temperature surfaces in ANUSPLIN. Fourth, the GIS-based methods are repeatable and could be applied to prepare maps for other areas. Finally, the GIS-based consumptive use map (or any of the input grids) can be combined with other GIS layers as they become available as well. Overall, our results show how GIS can be used to improve models, and they highlight the challenges of using highly generalized cartographic products with more detailed inputs in modern resource assessments.

In the second part of the study we generated a water supply sufficiency curve by examining the relationship between growing season water supply (deficit) and yield data for each of the 35 chosen soils across Montana. Regression models had similar shapes, and for 30 soils the coefficient of determination (R^2) was very high (>0.7). Averaging the slopes and intercepts for the 30 soils with high R^2 values resulted in a general yield - water deficit model. The sufficiency of water supply was derived from that general model. This new sufficiency was added as a factor in the original PI model. The PI model

was initially proposed as a way to determine the vulnerability of soils to productivity losses caused by erosion (soil removal) (Pierce et al., 1983, 1984a, 1984b). We applied the modified PI model to the 30 Montana soils used for model development to evaluate their vulnerability to soil loss and change in water deficit (climate change or fluctuation) as expressed in PI.

As expected, the modified PI was smaller than the original PI. The simulated removal of 10 cm of soil resulted in a 0-25 percent change in the modified PI (6 percent change on average). A change of this magnitude would occur over many decades since a soil erosion rate of 12 metric t/ha/yr is equal to the removal of approximately 1 cm of soil per decade. Soils with a high vulnerability to soil loss (largest change in modified PI) were usually thin soils. In contrast, a simulated increase in water deficit of 10 cm produced changes of 33-42 percent in the modified PI (36 percent change on average). This result indicates that the productivity is very sensitive to a 10 cm change in water supply in semi-arid landscapes like those found in Montana. It may also support findings of Pierce (1991) that the effects of erosion on productivity loss in any given year can be small relative to changes associated with annual variations in climate. The combined effect of simulated climate change or fluctuation and soil erosion losses (removal of 10 cm of soil in combined with an increase of 10 cm in water deficit) produced the largest change in modified PI, between 34 and 51 percent (an average of 41 percent change).

Furthermore, we used GIS to spatially illustrate: (1) the distribution of the modified productivity index estimates for Cherry silt loam on 2-8 percent slopes in Montana, and (2) the impact of simulated soil erosion and climate change on the

productivity of the Cherry silt loam series. Maps of modified PI show the spatial pattern/gradients of decreasing modified PI estimates from south to north and west to east. In addition, these maps show that the spatial coverage of lower modified PI values is larger than the coverage of higher estimates. Maps were generated to illustrate the spatial distribution of the effects of soil erosion and/or climate change on productivity, and indicate non-profitable/unproductive areas when a threshold PI value for crop production is assumed. Assuming a threshold of 0.3 for the simulations, 88 percent of the total area covered by the Cherry silt loam series would be unproductive/non-profitable when water deficit increased by 10 cm while all of the area would be productive if 10 cm soil eroded. Maps of such non-profitable/unproductive areas can be produced for each soil series. These results show that water supply has a major impact on crop production in semi-arid landscapes (as expected).

The type of model developed in this study is suited as a reconnaissance tool in semi-arid regions, especially in the developing world where data availability is a problem. This particular model has very modest data needs and a relatively simple conceptual basis (curves) and could be implemented easily in several GIS (Grid module of ARC/INFO, IDRISI , ARCVIEW Spatial Analyst Extension, GRASS, etc.). This offers advantages in terms of data (existing data could be used; e.g., topographic and climate database for Africa (Hutchinson et al., 1996)), ease of use (AML, AVENUE programs, etc.), and clarity of output. Maps can be produced showing areas that are more/less vulnerable to productivity losses caused by climate change and/or accelerated erosion. The coarse data used in the current study did not contain detailed enough spatial information to display all

of the agricultural soils of Montana in one map, and limits applications to region and state-wide analysis. We used the STATSGO soil database for the state of Montana in the current study because it provides the only spatial digital soil data that is currently available for the state. The STATSGO database is used primarily for river basin, multi-state, state, and multi-county resource planning, management, and monitoring (Mausbach et al., 1989; Reybold and TeSelle, 1989). STATSGO was created by generalizing detailed soil surveys and similar information. One mapping unit usually covers a large area and may contain up to 21 components (soil series).

Digital copies of the SSURGO database should be available for the state of Montana in about 2008 (Connie Williams, USDA-NRCS State Office, personal communication, 1997). SSURGO is used primarily for farm and ranch conservation planning, range and timber management, and county and parish, township, and watershed resource planning and management (Mausbach et al., 1989; Reybold and TeSelle, 1989). One mapping unit may contain up to three components (soil series). With this more detailed data, the spatial extent of each soil can be determined more precisely. We had to assume that the entire mapping unit in the STATSGO database contains one particular soil. With the finer data water deficit values may be confined to a different range of values and the sufficiency of water supply may be recalculated to generate more specific PI values. These PI values may indicate the areas that are most vulnerable to productivity losses or alternatively they might be used to identify areas where more detailed analysis needs to be performed. This could be a topic of a future study.

This study also suggests that there might be the following problems intrinsic in

the Montana Yield Model. First, by using different equations for each of the four consumptive water use areas relevant to crop production an artificial pattern/split (as opposed to a continuum) in yield estimates is produced. Second, our regression results indicate that predictions of yield estimates for cooler areas are more correct than for warmer areas. These results, combined with the availability of our spatially distributed continuous estimates of consumptive water use, show that revision of the yield model should be considered in future studies. The availability of the new consumptive water use estimates eliminates the need for four separate models. This option would allow the use of predicted CU values in each pixel and eliminate the need for the classification of CU prior to model implementation altogether. Alternatively, samples of yields across Montana for one or several crops could be related to our estimates of potential evapotranspiration to produce a new regression equation or model. These yield data are collected by farmers interested in precision farming with GPS and yield sensors attached to combines. A systematic effort is needed to collect and complete these data for a variety of scientific and management applications.

REFERENCES CITED

Baker, B.D., Gersmehl, P.J. (1991) Temporal trends in soil productivity evaluations. *The Professional Geographer* **43**, 304-318.

Blaney, H. F., Criddle, W. D. (1950) *Determining water requirements in irrigated areas from climatological and irrigation data.* Washington, D.C., United States Department of Agriculture, Soil Conservation Service Report No. TP-96, 48 pp.

Brown, D.A. (1993) Early nineteenth-century grasslands of the mid-continent plains. *Annals of the Association of American Geographers* **83**, 589-612.

Brown, P.L., Carlson, G.R. (1990) *Grain yields related to stored soil water and growing season rainfall.* Bozeman, MT, Montana State University, Agricultural Experiment Station, Special Report No.35, 22 pp.

Bryant, K.J., Lacewell, R D. (1989) Crop simulation models and economic analysis. In Clema, J. K. (ed.) *Proceedings of the 1989 Summer Computer Simulation Conference July 24-27, 1989*, Austin, TX, The Society, 723-737.

Caprio J.M., Nielsen, G.A. (1992) *Climate Atlas of Montana.* Bozeman, MT, Montana State University, Extension Service Bulletin No 113, 63 pp.

Carbone, G.J., Narumalani, S., King, M. (1996) Application of remote sensing and GIS technologies with physiological crop models. *Photogrammetric Engineering and Remote Sensing* **62**, 171-179.

Corbett, J.D., Carter, S.E. (1996) Using GIS to enhance agricultural planning: The example of inter-seasonal rainfall variability in Zimbabwe. *Transactions in GIS* **1**, 207-218.

Custer, S.G., Farnes, P., Wilson, J.P., Snyder, R.D. (1996) A comparison of hand- and spline-drawn precipitation maps for mountainous Montana. *Water Resources Bulletin* **32**, 393-405.

Doorenbos, J., Pruitt, W.O. (1977) *Crop water requirements.* Rome: UN Food and Agriculture Organization, Irrigation and Drainage Paper No. 24, Part I, 1-66.

Dumanski, J., Onofrei, C. (1989) Techniques of crop yield assessment for agricultural

land evaluation. *Soil Use and Land Management* **5**, 9-16.

Environmental Systems Research Institute, Inc. (ESRI, Inc.) (1997a) *ARC/INFO Version 7.1.1.* ESRI, Redlands, CA, Environmental Systems Research Institute, Inc.

Environmental Systems Research Institute, Inc. (ESRI, Inc.) (1997b) *ARC/VIEW Version 3.0a.* ESRI, Redlands, CA, Environmental Systems Research Institute, Inc.

Gantzer, C.J., McCarty, T.R. (1987) Predicting corn yields on a claypan soil using a soil productivity index. *Transactions of the American Society of Agricultural Engineers* **30**, 1347-1352.

Gersmehl, P.J., Brown, D.A. (1986) Regional differences in the validity of the concept of innate soil productivity. *Annals of the Association of American Geographers* **76**, 480-492.

Hutchinson, M.F. (1989a) *A new objective method for spatial interpolation of meteorological variables from irregular networks applied to the estimation of monthly mean solar radiation, temperature, precipitation, and windrun.* Canberra: Commonwealth Scientific and Industrial Research Organization, Division of Water Resources Technical Memorandum **89**, 95-104.

Hutchinson, M.F. (1989b) A procedure for gridding elevation and stream line data with automatic removal of spurious pits. *Journal of Hydrology* **106**, 211-232.

Hutchinson, M. F. (1991) *ANUDEM and ANUSPLIN User Guides.* Canberra: Australian National University, Centre for Resource and Environmental Studies Miscellaneous Report No. 91-1, 12 pp.

Hutchinson, M.F. (1995) Interpolating mean rainfall using thin plate smoothing splines. *International Journal of Geographical Information Systems* **9**, 385-403.

Hutchinson, M.F., Nix, H.A., McMahan, J.P., Ord, K.D. (1996) The development of a topographic and climate database for Africa. In: *Proceedings Third International Conference Integrating GIS and Environmental Modeling, Santa Fe, NM, 21-25 January 1996.* Santa Barbara, National Center for Geographic Information and Analysis, University of California, CD-ROM.

Kiniry, L.N., Scrivner, C.L., Keener, M.E. (1983) *A soil productivity index based upon predicted water depletion and root growth.* Columbia, MO, University of Missouri, Agricultural Experiment Station Research Bulletin No. 1051, 25 pp.

Larson, W.E., Pierce, F.J., Dowdy, R.H. (1983) The threat of soil erosion to long-term

crop production. *Science* **219**, 458-465.

Lindstrom, M.J., Schumacher, T.E., Jones, A.J., Gantzer, C.J. (1992) Productivity index model comparison for selected soils in north-central United States. *Journal of Soil and Water Conservation* **47**, 491-494.

Mausbach, M.J., Anderson, D.L., Arnold, R.W. (1989) Soil survey databases and their uses. In: *Proceedings of the 1989 Summer Computer Simulation Conference July 24-27, 1989*, Austin, TX, p. 659-664.

Montagne, C., Munn, L.C., Nielsen, G.A., Rogers, J.W., Hunter, H.E. (1982) *Soils of Montana*. Bozeman, MT, Montana State University, Agricultural Experiment Station, Bulletin No. 744, 95 pp.

Montana Agricultural Statistics Service (1996) *Montana Agricultural Statistics*. Helena, MT, Montana Agricultural Statistics Service, p. 12.

Neill, L.L. (1979) An evaluation of soil productivity based on root growth and water depletion. Columbia, MO, Unpublished M.S. Thesis, Department of Agronomy, University of Missouri.

Olson, K.R., Lal, R., Norton, L.D. (1994) Evaluation of methods to study erosion-productivity relationships. *Journal of Soil and Water Conservation* **49**, 586-590.

Pierce, F.J. (1991) Erosion productivity impact prediction. In Lal, R., Pierce, F.J. (eds) *Soil Management for Sustainability*. Ankeny, IO, Soil and Water Conservation Society, p. 35-52.

Pierce, F.J., Larson, W.E., Dowdy, R.H., Graham, W.A.P. (1983) Productivity of soils: Assessing long-term change due to erosion. *Journal of Soil and Water Conservation* **38**, 39-44.

Pierce, F.J., Dowdy, R.H., Larson, W.E., Graham, W.A.P. (1984a) Soil productivity in the Corn Belt: An assessment of erosion's long-term effects. *Journal of Soil and Water Conservation* **39**, 131-138.

Pierce, F.J., Larson, W.E., Graham, W.A.P. (1984b) Soil loss tolerance: Maintenance of long-term soil productivity. *Journal of Soil and Water Conservation* **39**, 136-138.

Pierce, F.J., Larson, W.E., Dowdy, R.H. (1984c) Evaluation of soil productivity in relation to soil erosion. In F.R. Rijsberman, Wolman M.G. (eds.) *Quantification*

of the Effect of Erosion on Soil Productivity in an International Context. Delft, The Netherlands, Delft Hydaulics Laboratory: 157 pp. (p.53-69)

Reybold, W.U., TeSelle, G.W. (1989) Soil geographic data bases. *Journal of Soil and Water Conservation* **44**, 28-29.

Rijsberman, F.R., Wolman, M.G. (1985) Effect of erosion on soil productivity: An international comparison. *Journal of Soil and Water Conservation* **40**, 349-354.

SAS Institute, Inc. (1997) *SAS Version 6.12.* Cary, NC, SAS Institute, Inc.

United States Department of Agriculture, Natural Resource Conservation Service (USDA-NRCS) (1994) *State Soil Geographic (STATSGO) Data Base. Data use information.* Washington, D.C., United States Department of Agriculture, Natural Resources Conservation Service, National Soil Survey Center. Miscellaneous Publication No. 1492, 37 pp.

United States Department of Agriculture, Soil Conservation Service (USDA-SCS) (1988) *Montana Irrigation Guide.* Bozeman, MT, Montana SCS State Office, 360 pp.

United States Department of Agriculture, Soil Conservation Service (USDA-SCS) (1993) *National Engineering Handbook. Part 623. Irrigation Water Requirements.* Washington, D.C., U.S. Department of Agriculture, Soil Conservation Service: 2-227-2-258.

Usery, E.L., Pocknee, S., Boydell, B. (1995) Precision farming data management using geographic information systems. *Photogrammetric Engineering and Remote Sensing* **61**, 1383-1391.

Williams, J.R., Renard, K.G., Dyke, P.T. (1983) EPIC: A new method for assessing erosion's effect on soil productivity. *Journal of Soil and Water Conservation* **38**, 381-383.

Wilson, J.P., Sandor, S.P., Nielsen, G.A. (1991) Productivity Index model modified to estimate variability of Montana small grain yields. *Soil Science Society of America Journal* **55**, 228-234.

Wilson, J.P., Gerhart, K.E.S., Nielsen, G.A., Ryan, C.M. (1992) Climate, soil and crop yield relationships in Cascade County, Montana. *Applied Geography* **12**, 261-270.